

INJECTION LOCKED F-P LD IN
WDM-PON

INJECTION LOCKED FABRY-PEROT LASER DIODE IN WAVELENGTH DIVISION MULTIPLEXING PASSIVE OPTICAL NETWORK

By

YUDAN YAN, M. Sc.

July, 2008

A Thesis Submitted to the School of Graduate Studies in Partial Fulfillment of the
Requirements for the Degree of Master of Applied Science

McMaster University

© Copyright by Yudan Yan, October 2008

MASTER OF APPLIED SCIENCE (2008) McMaster University (Electrical &
Computer Engineering) Hamilton, Ontario

TITLE: Injection-Locked Fabry-Perot Laser Diode
In Wavelength Division Multiplexing Passive
Optical Network

AUTHOR: Yudan Yan, M. Sc. (Nanjing University of
Post and Telecom, China)

SUPERVISOR: Dr. Wei-Ping Huang, Professor

NUMBER OF PAGES: xi, 71

Abstract

The bandwidth demanding in the access network has been increasing rapidly over the past several years. The predominant broadband access network solutions deployed today are digital subscriber line (DSL) and community antenna television (CATV) (cable TV) based networks. However, the passive optical network (PON) which is a point to multipoint access network based on optical fibers provides much higher bandwidth compared to current access networks based on copper lines.

Incorporating wavelength division multiplexing (WDM) in a PON allows a much higher bandwidth compared to the standard PON which operates in the single wavelength mode where the one wavelength is used for upstream transmission and another different wavelength is used for downstream transmission. Moreover, WDM-PON offers the advantages in terms of capacity, low latency and service transparency. In the past five years WDM-PON technology has been developed to a mature for commercial consideration.

In this thesis, we start from some fundamentals about WDM-PON and the technology challenge for WDM-PON which is to avoid the need for expensive wavelength selective optical components in the end-user optical network unit (ONU). Then we investigate Injection Locked Fabry-Perot Laser Diode with narrow band amplified spontaneous emission (ASE) noise as an approach to be a wavelength independent ONU. We study its theoretical model and compare the experimental results with the simulation results based on the theoretical model.

Acknowledgements

I would like to express my highest appreciation to my supervisor, Dr. Wei-Ping Huang, whose guidance, support and encouragement made this work possible to be completed. His diverse insights and pivotal ideas lead me to the frontier of photonics; from him, I have learnt the creativity and rigorousness in research.

I greatly appreciate the assistance I received from my committee members, Dr. Xun Li and Dr. Chang-Qing Xu. Their constructive criticism and valuable advice on numerical and physical modeling helped me a lot in this study. I am also very thankful to Dr. Xiaobin Hong and doctor candidate Yanping Xi for their wholesome directions and comments throughout my work.

I would like to say many thanks to my colleagues in the Photonic Research Group for their help and friendship. They made a direct contribution in this thesis by proofreading it. I would also like to thank the administrative and technical staffs in Department of Electrical and Computer Engineering for their tireless effort and helpful attitude.

Last but not least, I would like to thank my best friend, Elise for her consistent help. I would like to thank my husband, Shiming for his endless love and support in my life. I also want to thank my son, Jack for his warm heart and his love.

2.2 Injection locked Fabry-Perot Laser Diode.....	22
2.3 Summary.....	35
Chapter3. Narrow Band Amplified Spontaneous Emission.....	37
3.1 Spectral sliced Amplified Spontaneous Emission.....	37
3.2 Summery	40
Chapter4. Experiments for Injected-Locked FP-LD with NASE.....	41
4.1 Introduction.....	41
4.2 Experiments.....	42
Chapter5. Simulation for Injection Locked F-P LD with NASE.....	47
5.1 Introduction.....	47
5.2 Simulation Results.....	52
5.3 Summary.....	64

Chapter6. Summary and Future work	65
References.....	68

List of Figures

Figure 1-1 Simple WDM-PON architecture.....	3
Figure 1-2 Coring SMF-28 Optical Fiber.....	6
Figure 1-3 Dispersion of Coring SMF-28.....	7
Figure 1-4 Reflective architecture in WDM-PON.....	8
Figure 2-1 Fig.2-1 F-P LD infrastructure.....	10
Figure 2-2 Fig.2-2 longitudinal modes traveling within the cavity.....	11
Figure 2-3 Fig.2-3 Characteristics of F-P LD.....	12
Figure 2-4 Fig.2-4 RIN of F-P LD.....	14
Figure 2-5 Intensity noise spectrums for several power levels.....	16
Figure 2-6 Diagram of Injection Locked.....	23
Figure 2-7 spectra of AlGaAs heterostructure laser modulated by 500Mbit/s.....	28
Figure 2-8 power ratio between injected mode and lasing mode and side modes	28
Figure 2-9 locking range of LD with respect to gain.....	31
Figure 2-10 time evolution of carrier density and photon population under relaxation oscillation.....	32
Figure 2-11 relation between RIN and detuning when line width enhancement factor is small.....	35
Fig.3-1 F-P LD injected locked by sliced ASE in the reflective architecture in WDM-PON.....	38

Figure 4-1 diagram about experiment setup.....	42
Figure 4-2 measured spectrum of ASE injected F-P LD (1).....	45
Figure 4-3 measured spectrum of ASE injected F-P LD (2).....	46
Fig.5-1 Power output distribution in the free running F-P LD.....	53
Fig.5-2 Total power output distribution in the free running F-P LD.....	53
Fig.5-3 Carrier density in free running F-P LD.....	54
Fig. 5-4 Power distributions in the free running F-P LD.....	54
Fig.5-5 Power distributions in the injection locked F-P LD with -50dBm ASE injection.....	55
Fig. 5-6 Power distributions in the injection locked F-P LD with -35dBm ASE injection.....	55
Fig. 5-7 Power distributions in the unlocked F-P LD with -18.8dBm ASE injection.....	56
Fig. 5-8 Power distributions in the injection locked F-P LD with -18.5dBm ASE injection.....	56
Fig.5-9 Power distributions in the injection locked F-P LD with -10dBm ASE injection.....	56
Fig. 5-10 Power distributions in the injection locked F-P LD with -3dBm ASE injection.....	57
Fig. 5-11 Power in the injection locked F-P LD with 10dBm ASE injection.....	57
Fig. 5-12 RIN in the free running F-P LD.....	58

Fig. 5-13 RIN in the injection locked F-P LD with -50dBm ASE injection.....	58
Fig. 5-14 RIN in the injection locked F-P LD with -35dBm ASE injection.....	59
Fig. 5-15 RIN in the injection locked F-P LD with -18.8dBm ASE injection.....	59
Fig. 5-16 RIN in the injection locked F-P LD with -18.5dBm ASE injection.....	60
Fig.5-17 RIN in the injection locked F-P LD with -10dBm ASE injection.....	60
Fig. 5-18 RIN in the injection locked F-P LD with -3dBm ASE injection.....	61
Fig.5-19 RIN in the injection locked F-P LD with 10dBm ASE injection.....	61
Fig.5-20 Gain in the free running F-P LD.....	62
Fig.5-21 Gain in the injection locked F-P LD with -50dBm ASE injection.....	62
Fig.5-22 Gain in the injection locked F-P LD with -35dBm ASE injection.....	62
Fig.5-23 Gain in the injection locked F-P LD with -18.8dBm ASE injection.....	62
Fig.5-24 Gain in the injection locked F-P LD with -18.5dBm ASE injection.....	63
Fig.5-25 Gain in the injection locked F-P LD with -10dBm ASE injection.....	63
Fig.5-26 Gain in the injection locked F-P LD with -3dBm ASE injection.....	63
Fig.5-27 Gain in the injection locked F-P LD with 10dBm ASE injection.....	64
Fig.6-1 Proposed WDM-PON architecture using CW-injection-locked F-P L....	64

List of Tables

Table 1-1 Optical Fiber Spectral Bands.....	2
Table 1-2 PON technologies.....	4
Table 1-3 Channel / Wavelength Reference Sheet for ITU-T G.694.1	5
Table 4-1 light powers at reference points.....	44
Table 5-1 Physical parameters of F-P LD.....	51

Chapter1. Introduction

1.1 Background for WDM-PON

Passive Optical Network (PON) technology is originally developed in 1980's [1] as a cost effective way sharing fiber infrastructure for the narrowband telephony to business premises. Since then PONs have moved on to interactive broadband communications implemented as BPON (ITU-T G.983), EPON (IEEE 802.3ah) and the current GPON (ITU-T G.984) [2].

All these systems are based on Time Division Multiplexed Access (TMDA) and satisfy Fiber-to-the-Home (FTTH) standard. Recently people also realize that wavelength Division Multiplexing (WDM) offers the alternative method of sharing PON capacity among multiple users and offers advantages in terms of capacity, low latency and service transparency (See Table 1-1 PON technologies [3]). It is widely believed that the WDM-PON would be the next generation of PONs.

	A/BPON	EPON (GEPON)	GPON	10 GEPON	WDM PON
Standard	ITU G.983	IEEE802ah	ITU G.984	IEEE P802.3av	Not yet

Data Packet Cell Size	53 bytes	1518 bytes	53 to 1518 bytes	1518 bytes	Independent
Maximum Downstream Line Rate	622 Mbps	1.2 Gbps	2.4 Gbps	IP; 2.4 Gbps, Broadcast; 5 Gbps On-demand; 2.5 Gbps	1-10 Gbit/s per channel
Maximum Upstream Line Rate	155/622 Mbps	1.2 Gbps	1.2 Gbps	2.5 Gbps	1-10 Gbit/s per channel
Downstream wavelength	1490 and 1550 nm	1550 nm	1490 and 1550 nm	1550 nm	Individual wavelength/channel
Upstream wavelength	1310 nm	1310 nm	1310 nm	1310 nm	Individual wavelength/channel
Traffic Modes	ATM	Ethernet	ATM Ethernet or TDM	Ethernet	Protocol Independent
Voice	ATM	VoIP	TDM	VoIP	Independent
Video	1550 nm overlay	1550 nm overlay/IP	1550 nm overlay/IP	IP	1550 nm overlay/IP
Max PON Splits	32	32	64	128	16/100's
Max Distance	20 Km	20 Km	60 Km	10 Km	20 Km
Average Bandwidth per User	20 Mbit/s	60 Mbit/s	40 Mbit/s	20 Mbit/s	Up to 10 Gbit/s

(Table 1-1 PON technologies)

Fig.1-1[3] is the infrastructure of WDM-PON (Full Service Access Network (FSAN) WDM-PON standard is expected to be finalized by 2010). WDM-PON deploys a separate wavelength channel from the Optical Line Terminal (OLT) to each Optical Network Unit (ONU) for each of the upstream and downstream directions. This approach creates a point-to-point link between

the OLT and each ONU which can operate the full bit rate of wavelength channel. And different sets of wavelength may support different independent PON sub networks because different wavelength may be operated at different bit rates. All the operations are over the same fiber infrastructure.

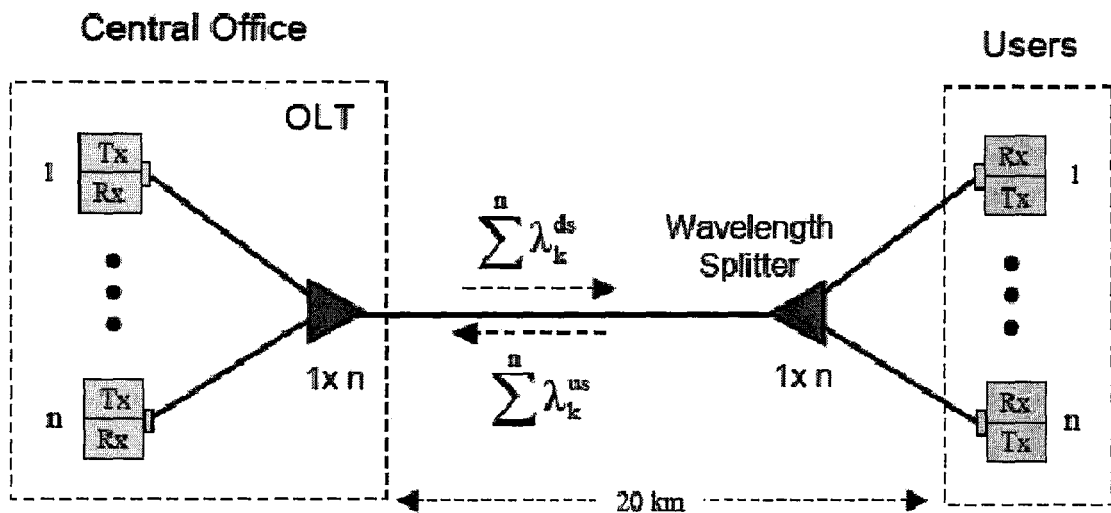


(Fig.1-1 Infrastructure of WDM-PON)

In traditional long haul WDM network, wavelength spacing of more than 20nm is generally called coarse WDM (CWDM) (ITU-T G.695). Wavelength spacing less than 3.2nm is typically called Dense WDM (DWDM) (ITU-T G.694). Recently the ITU defined the following spectral bands (Table 1-2) in order to clarify the terminology that is used for optical fiber systems. These definitions are

meant for classification purposes only.

Band	Descriptor	Range (nm)
O band	Original	1260 to 1360
E band	Extended	1360 to 1460
S band	Short wavelength	1460 to 1530
C band	Conventional	1530 to 1565
L band	Long wavelength	1565 to 1625
U band	Ultra long wavelength	1625 to 1675

(Table 1-2: Optical Fiber Spectral Bands)

Table 1-3 is the Channel / Wavelength Reference Sheet for ITU-T G.694.1 (100GHz Grid) in DWDM system in C band. The wavelength grid is around 0.8nm.

Channel No.	Wavelength (nm)	Frequency (THz)	Channel No.	Wavelength (nm)	Frequency (THz)
61	1528.77	196.10	38	1546.92	193.80
60	1529.55	196.00	37	1547.72	193.70
59	1530.33	195.90	36	1548.51	193.60
58	1531.12	195.80	35	1549.32	193.50
57	1531.9	195.70	34	1550.12	193.40
56	1532.68	195.60	33	1550.92	193.30
55	1533.47	195.50	32	1551.72	193.20
54	1534.25	195.40	31	1552.52	193.10
53	1535.04	195.30	30	1553.33	193.00
52	1535.82	195.20	29	1554.13	192.90
51	1536.61	195.10	28	1554.94	192.80

50	1537.4	195.00	27	1555.75	192.70
49	1538.19	194.90	26	1556.55	192.60
48	1538.98	194.80	25	1557.36	192.50
47	1539.77	194.70	24	1558.17	192.40
46	1540.56	194.60	23	1558.98	192.30
45	1545.35	194.50	22	1559.79	192.20
44	1542.14	194.40	21	1560.61	192.10
43	1542.94	194.30	20	1561.42	192.00
42	1543.73	194.20	19	1562.23	191.90
41	1544.53	194.10	18	1563.05	191.80
40	1545.32	194.00	17	1563.86	191.70
39	1546.12	193.90			

(Table 1-3 Channel / Wavelength Reference Sheet for ITU-T G.694.1
(100GHz Grid))

1.2 Wavelength independent ONU

WDM-PON is a kind of single mode optical fiber communication system considering its high capacity of GHz level. And in this thesis we only consider DWDM-PON since we will study the characteristics which satisfy the requirements of WDM-PON network.

However, since WDM-PON is an also kind of FTTH network which is price sensitive, in practice the type of laser currently used in the long haul DWDM transmission is cost prohibitive when using in the WDM-PON. Another difference from WDM is that WDM network scopes expect more than 100kms but WDM-PON network scopes are normally within 20kms (See Table 1-1).

Let's study how optical fibers affect the network performance within 20kms. We choose ITU G.652.D standard compatible optical fibers (Corning SMF-28), which is recommended as the leading solution as communication fibers in new FHHT network by Corning [4].

Fig.1-2[4] shows Corning SMF-28 optical fibers. It shows the attenuation in S-band, C-band and L-band, where the water peak is, is less than 10dB within 20kms. C-band has the smallest attenuation.

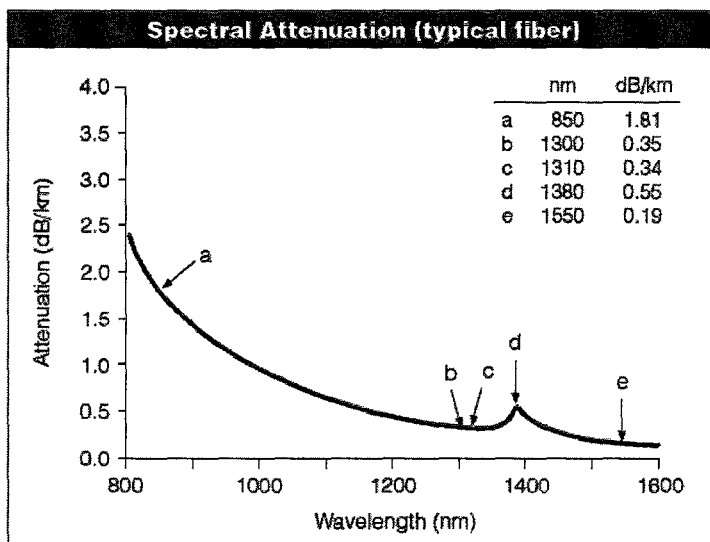


(Fig.1-2 Corning SMF-28 optical fiber)

Then let's take a look at dispersion of Corning SMF-28:

the zero dispersion Slope: $S_0 \leq 0.092 \text{ps}^2/\text{nm}^2 \cdot \text{km}$

the zero dispersion wavelength: $1301.5\text{nm} \leq \lambda_0 \leq 1321.5\text{nm}$

Dispersion $D(\lambda) \approx \frac{S_0}{4} \left[\lambda - \frac{\lambda_0^2}{\lambda} \right] \text{ps}^2/\text{nm} \cdot \text{km}$ (1)

here λ is working wavelength $1200 \text{ nm} \leq \lambda \leq 1600 \text{ nm}$

Fig.1-3 is plotted from equation (1) by associated parameters. Roughly calculated, the dispersion in working spectrum is between $-13 \text{ ps/nm} \cdot \text{km}$ to $20 \text{ ps/nm} \cdot \text{km}$. Thus the total dispersion is between -260 ps/nm to 400 ps/nm within 20kms. C-band's dispersion is not as good as other band but still within the system tolerance.

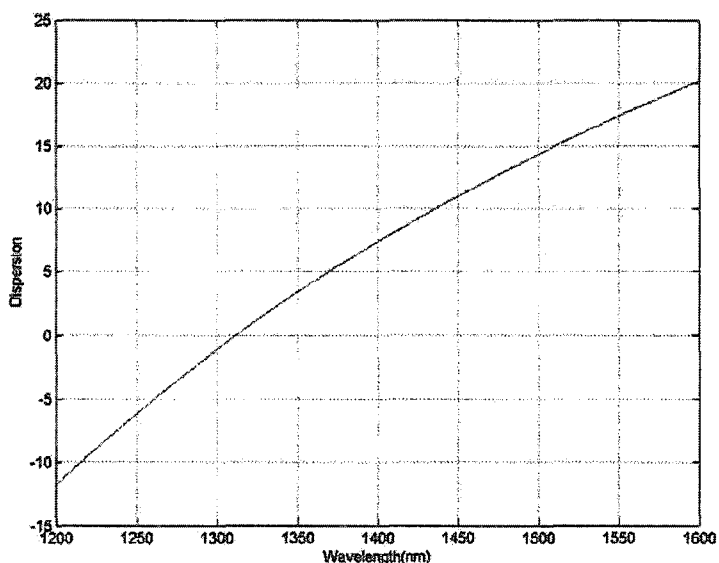


(Fig.1-3 Dispersion of Coring SMF-28)

If we only consider effects from the fibers, C-band is the best work space for upstream light signal in WDM-PON.

Fig.1-1 shows that cost for a single WDM-PON network include:

- 1) One OLT which dedicate different wavelengths to each ONU
- 2) One Remote Node wavelength splitter

- 3) n * ONU each of which has its own transmitter and receiver.
- 4) Optical Fibers

OLT and wavelength splitter are in the central office and are shared by multiple end users. Then the technology challenge about WDM-PON will be to avoid expensive wavelength selective optical components in each end-users optical network unit (ONU). Thus the ONU which satisfies wavelength independence, in other words, colorless ONU must be used.

A tunable laser satisfies the requirement of a colorless ONU but at present the price of it is still far too high.

Another alternative technology recently was considered to reduce the cost of WDM-PON by eliminating the wavelength-specific sources and replacing them with low-cost identical F-P LD. All the transmitters are identical but they operate at different DWDM wavelengths by using an automatic injection-locked scheme.

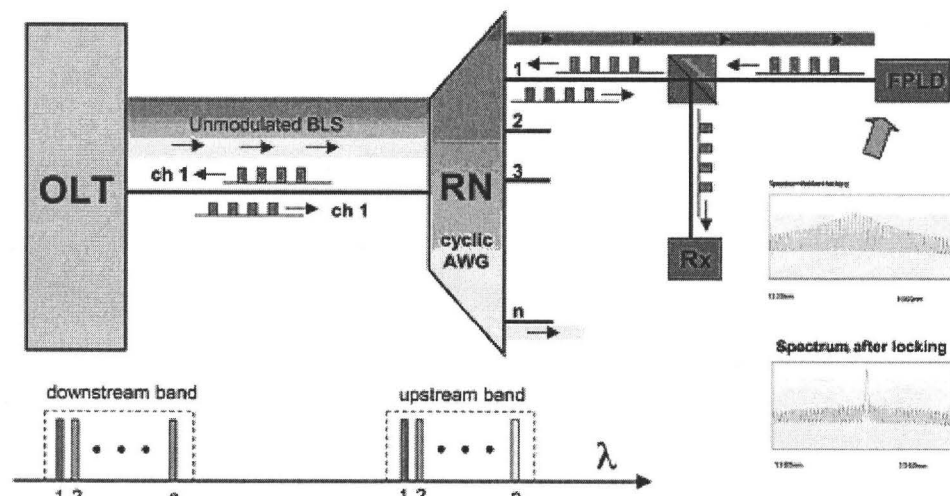


(Fig.1-4 WDM-PON with injection locked as ONU transmitter)

Fig.1-4[3] illustrates the basic principle for WDM-PON using external injection locked F-P LD. An un-modulated external optical beam is injected into

the cavity of F-P LD after sliced by a Array Wavelength Grating (AWG) which acts as a de-multiplexer then modulated by the user bandwidth and goes back to the central office through the same AWG which works as a multiplexer and band pass filter.

Recently there are many reports about experimentally demonstrating injection locked F-P LD as wavelength independent transmitter in ONU. In South Korea, expensive WDM-PON trail network based on injection locked F-P LD has been successfully deployed. However, theoretical study about injection locked F-P LD doesn't go as fast as its experimental study.

1.3 Thesis outline

In this paper we highlight Injection Locked Fabry-Perot Laser Diode injected by narrow band ASE (NASE) noise as an approach to be a wavelength independent ONU. We study a theoretical model of injection locked F-PLD based on the rate equations for the semiconductor laser diode. We simulate the F-P LD using MATLAB by solving the rate equations numerically. The parameters of F-P LD are chosen partly from experiments, partly from the typical parameters of F-P LD. Then we compare the experimental results with the simulation results based on the theoretical model.

Chapter2. Injection Locked F-P LD

2.1 Fabry-Perot Laser Diode

F-P LD is a semiconductor laser diode in which two mirrors are separated by an amplifying medium with an inverted population, making an F-P LD cavity. F-P LD is the most common type of laser diode and is the most economical, but it is generally slower and noisier than others such as distributed feedback (DFB) lasers. F-P LD is an edge-emitting laser (See Fig.2-1).

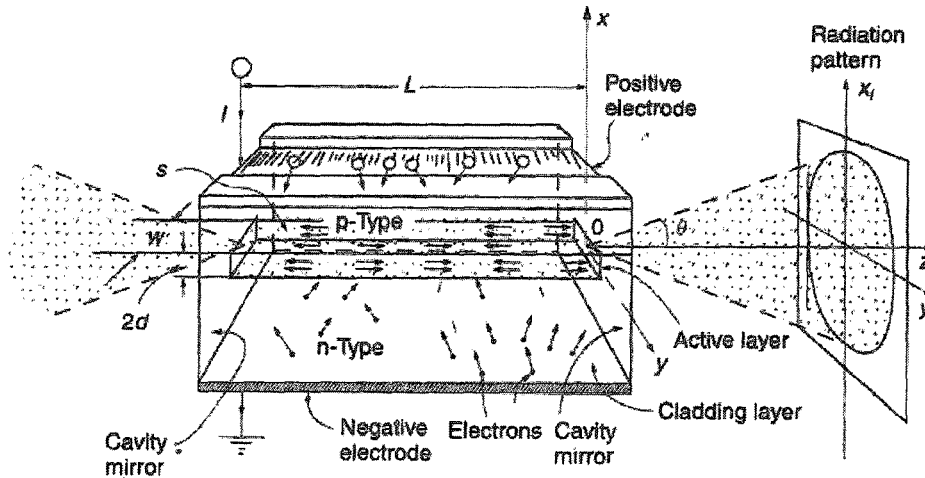


(Fig.2-1 F-P LD infrastructure)

Fig.2-2 depicts the longitudinal mode travelling within the cavity. Wavelengths of the longitudinal modes are selected by the cavity length according to the following equation:

$$2L = N\lambda \quad (2)$$

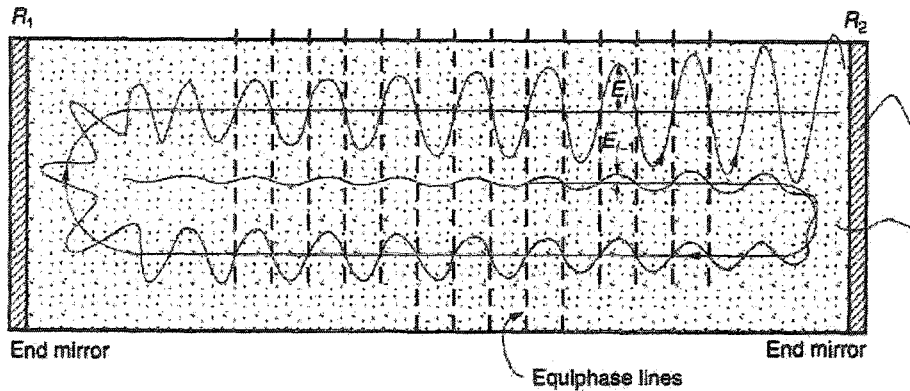


(Fig.2-2 longitudinal mode travelling within the cavity)

L is the cavity length; λ is the longitudinal wavelength and N is arbitrary integral. F-P LD cavity can support an infinite number of modes theoretically. However, the semi-conductor material provides gain only within a narrow range of wavelengths according to the following equation:

$$\lambda = hc/E_g \quad (3)$$

where h is Planck's constant and E_g is the band gap energy of the particular active gain medium associated with the laser diode.

The Fresnel reflection from the facets (which become the laser end mirrors) due to the light traversing from active optical materials with index of refraction about 3.25 to air whose index of refraction is about 1.0. If a different reflectance is required, the facets must be coated with relative refraction materials to change the reflectance.

Like most typical semiconductor lasers, F-P LD has almost all the

common characteristics about semiconductor LD. Fig.2-3-a and Fig.2-3.b show the cross section of F-P LD and relation between light output versus DC bias current.

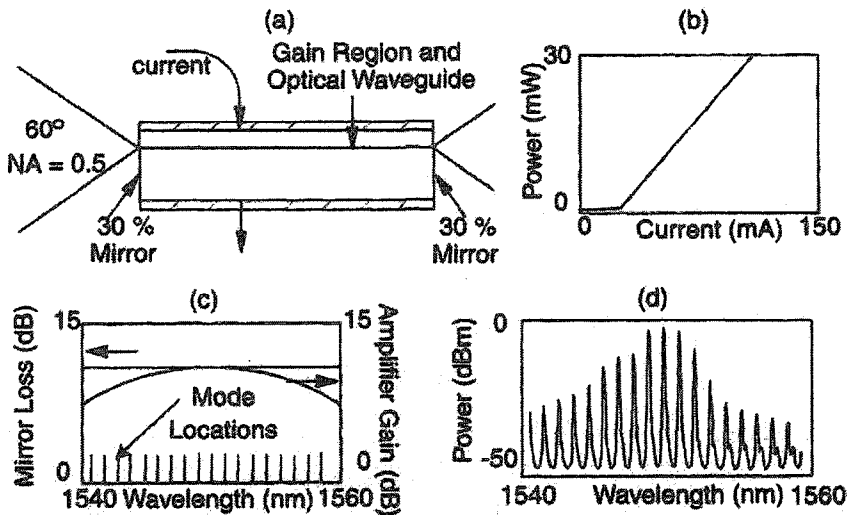


(Fig.2-3 Characteristics of F-P LD)

Fig.2-3-c shows relation between the line width of the gain curve and the longitudinal modes. The gain line width is typically about 7nm to 20nm wide, while the longitudinal mode spacing is about 2nm. The result is the spectrum seen in Fig.2-3-d above where the longitudinal modes are modified by the gain curve.

Laser power and frequency are expected to be constant in optical fiber communication system. But in reality, laser output exhibits intensity as well as phase fluctuations. Basically the origin of these fluctuations lies in the quantum nature of the lasing process. In general, intensity noise reaches its peak in the vicinity of the laser threshold and then decreases rapidly with an increase in the drive current. Thus the intensity noise spectrum shows a peak near the relaxation

oscillation frequency as a consequence of the laser's intrinsic resonance. Phase fluctuation produce spectral broadening of each longitudinal mode and is responsible for the observed line width.

Noises of F-P LD mainly come from the quantum effects of spontaneous emission, random carrier generation and recombination which trigger unstable oscillations in semiconductor lasers. Langevin studied these random noise effects and called them Langevin noises [5]. And Langevin noises are defined for the photon number in laser oscillations so we will study rate equations associated inverse change of photon density and carrier density later.

Relative intensity noise (RIN) is to measure the relative noise level to the average DC signal power which is detected by a high speed photo receiver from the light output from a semiconductor laser as an electric signal. Theoretically RIN describes the inverse carrier-to-noise-ratio: the ratio of the mean-square optical intensity noise to the square of the average optical power [5].

The optical output power of the laser in a certain frequency can be considered to be:

$$P(f) = P + \Delta P \quad (4)$$

P is an average value and ΔP is a fluctuating quantity with zero mean value then the RIN can be described as:

$$RIN = \frac{\langle \Delta P^2 \rangle}{P^2} \quad (5)$$

Where $\langle \Delta P^2 \rangle$ is the mean-square optical intensity fluctuation (in a certain

bandwidth such as one Hz) at a specified frequency and P is the average optical power.

Fig.2-4 is a typical RIN of F-P LD measured by Agilent [6].

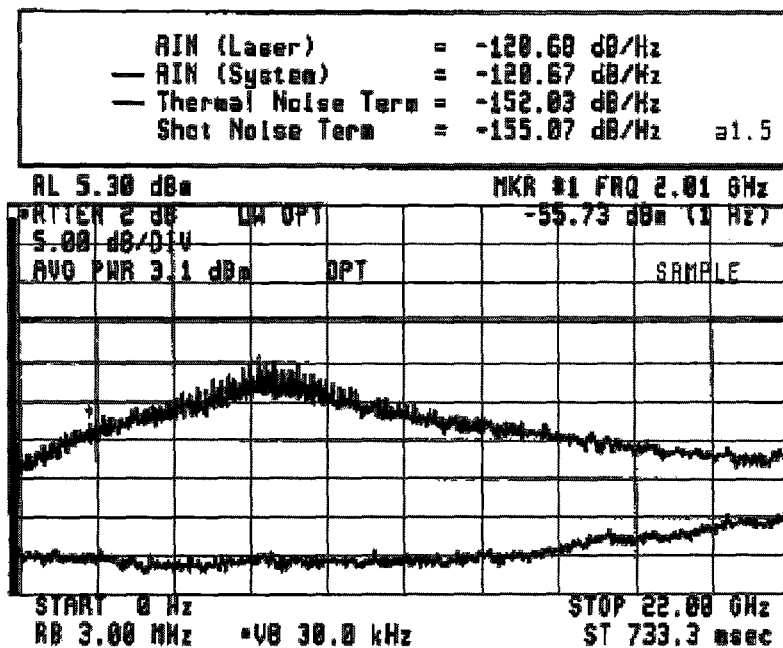


(Fig.2-4 RIN of F-P LD)

In semiconductor laser diode, there is an important parameter: line width enhancement factor which depicts the complex susceptibility of the medium at laser oscillation.

$$\alpha = \frac{\text{Re}\{X_p\}}{\text{Im}\{X_p\}} \quad (6)$$

X_p is the complex susceptibility.

Since the line width enhancement factor of other lasers, such as gas lasers, is almost equal to zero, while it has a non-zero value for semiconductor lasers and

usual between 3 and 7 (demonstrated by Cook 1975, and Osinski and Buss 1987) [7], it becomes the specific characteristic of semiconductor laser other than other type of lasers. It was then later found by Henry (1982)[7] that the increased line width results from a coupling between intensity and phase noise, by a dependence of the refractive index on the carrier density in the semiconductor laser.

The spectral line width of laser oscillations is calculated from the well-known Schalow-Townes equation. The half-width of full maxima (HWFH) of the longitudinal single mode laser diode is calculated as the following [7]:

$$\Delta f = \frac{\lambda \omega^2}{4\pi P} (1 + \alpha^2) \quad (7)$$

The line width of gas lasers is negligible because α is almost zero. Semiconductor lasers have a non-negligible value of the α parameter and the line width of semiconductor lasers is $(1 + \alpha^2)$ times larger than that of ordinary lasers (Henry 1982, 1983, and 1986, Petermann 1988, and Agrawal and Dutta 1993) [7]. The spectral line width of laser oscillations decreases with an increase of the photon rate, so that the line width becomes narrow with an increase of the laser output power. Fig.2-5 is Intensity spectrum for several power level numerically calculated by Henry in 1986[7].

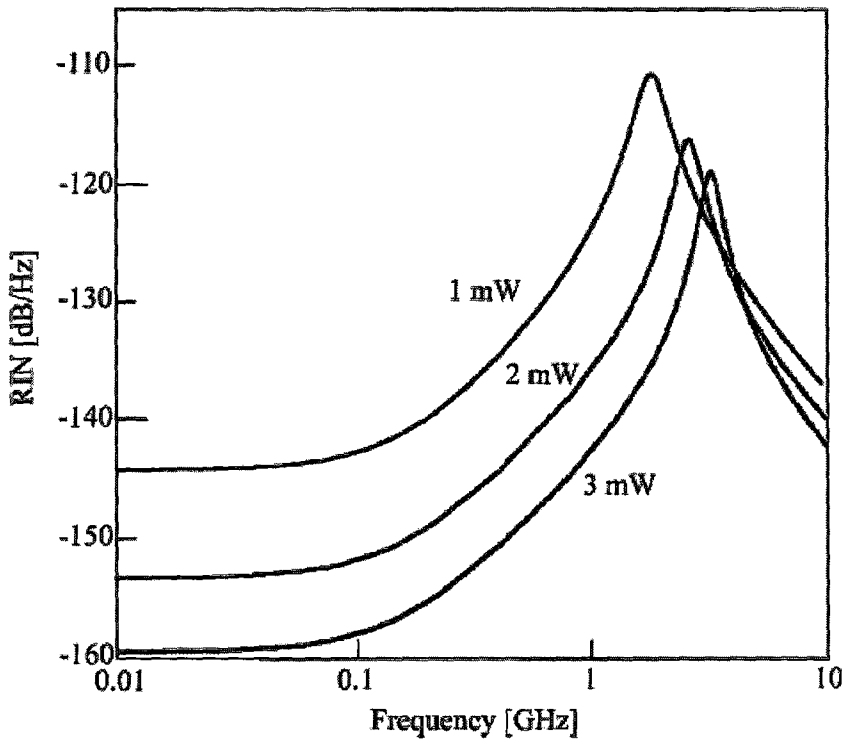


(Fig.2-5 Intensity spectrum for several power levels)

Here P is the photon density and R_{sp} is given in equation (30).

The static, dynamic and spectral characteristics of F-P LD can be described by rate equation model [8] as below. We start from Maxwell's equations:

$$\nabla^2 \mathbf{E} - \frac{1}{c^2} \frac{\partial^2 (\epsilon \mathbf{E})}{\partial t^2} = 0 \quad (8)$$

We assume that the equation works for a fast response semiconductor so we only consider ϵ' of the complex dielectric constant as the loss but we don't consider its induced polarization.

The optical field \mathbf{E} in general may consist of a large number of lateral,

transverse and longitudinal modes oscillating at different frequency. Each mode forms a standing-wave pattern in the axial direction arising from a superposition of the forward and backward running waves. For simplicity, we assume that the laser structure has been designed to support a single lateral, transverse and longitudinal mode. Then \mathbf{e} can be expressed as:

$$\mathbf{e}(x, y, z, t) = \frac{1}{2} \mathcal{R}\Phi(x)\Psi(y)\sin(kz)E(t)\exp(-i2\pi ft) + c. c. \quad (9)$$

The sinusoidal variation of the optical field in the z direction assumes facets with high reflectivity. Wave number k is associated with equation (2) and given by:

$$k = \frac{n2\pi f}{c} \quad (10)$$

$$k_0 = \frac{2\pi f}{c} \quad (11)$$

L is the cavity length; f is the cavity resonance frequency; n is the refractive index which changes with external pumping with:

$$n \cong n_b + \Delta n \quad (12)$$

$$n_b = \sqrt{\epsilon_b} \quad (13)$$

n_b is the background refractive index of the un-pumped material and ϵ_b is the background dielectric index of un-pumped material.

Δn is the amount by which it changes in the process of charge carriers and is given by

$$\Delta n = \text{Re}(\chi_p)/2n_b \quad (14)$$

Here χ is a second rank tensor given by

$$\chi = \chi_0 + \chi_p \quad (15)$$

to emphasize the dispersive nature of medium response. χ_0 is the medium susceptibility and χ_p is contributed by strength of external pumping. Both χ_0 and χ_p are complex.

We also assume $E(\mathbf{r}, t)$ varies slowly multiple by $\Phi(x)$ and $\Psi(y)$, and integrated the whole x and y . After some simplicity [8], we can get:

$$\frac{dE}{dt} = \frac{in}{n_g} (2\pi f_{mode} - 2\pi f) E + \frac{i2\pi f_{mode}}{n_g} (\Gamma \Delta n + i\alpha/2k_0) E \quad (16)$$

Where Γ is the confinement factor; f_{mode} is laser mode; n is mode index ; n_g is the group refractive index; Δn is the carrier induced index change

$$\Delta n = -\left(\frac{\alpha}{2k_0}\right) \Delta g \quad (17)$$

Where

$$\Delta G = \Gamma v_g \Delta g = G - \gamma \quad (18)$$

In the formulations, α is the line width enhancement factor defined in equation (6) and (17) which provides a proportionality between the gain and index changes; γ is explained in equation (27).

Equation (19) [8] shows that gain changes from its threshold value and the phase changes as well.

$$\frac{d\varphi}{dt} = -(2\pi f_{mode} - 2\pi f_{th}) + \frac{1}{2} \alpha (G - \gamma) \quad (19)$$

Physically this is so because a gain change is always accompanied by an index change that shifts the longitudinal mode frequencies. f_{th} corresponds to the threshold value of the mode index. By expanding f_{mode} in the vicinity of f_{th} , we can get:

$$\left(\frac{n}{n_g}\right) (2\pi f_{mode} - 2\pi f) = 2\pi f_{mode} - 2\pi f_{th} \quad (20)$$

$\bar{\alpha}$ is the mode absorption coefficient given by

$$\bar{\alpha} = -\Gamma g + \alpha_{int} + \alpha_m \quad (21)$$

Since photon density is defined as [8]:

$$P = \frac{1}{2} \frac{\epsilon_0 n_g^2}{2\pi f_0 h} |e|^2 = |E|^2 \quad (22)$$

$$E = \sqrt{P} \exp(-i\varphi) \quad (23)$$

Substitute (19), (22), (23) into (16), considering Langevin noise and multi-mode oscillation in cavity, we can get rate equation to describe time evolution of carrier density and photon intensity in cavity [8]. We study rate equation with photon density just because Langevin noises are defined by photon number.

$$\frac{dP_i}{dt} = (G_i - \gamma)P_i + R_{sp}(\omega_i) + F_P(t) \quad (24)$$

$$\frac{dN}{dt} = \frac{I}{qV} - \gamma_s N - \frac{\sum_i G_i P_i}{V} + F_N(t) \quad (25)$$

$$\frac{d\varphi}{dt} = 2\pi(f_i - f_{th}) + \frac{1}{2}\alpha(G_i - \gamma) + F_\varphi(t) \quad (26)$$

i is i-th mode; V is the volume of active region of cavity.

γ is photon decay rate that can be used to define the photon lifetime τ_P :

$$\gamma = \gamma_g(\alpha_{int} + \alpha_m) = \tau_g^{-1} \quad (27)$$

$$\alpha_m = \frac{1}{2L} \cdot \ln\left(\frac{1}{R_f R_r}\right) \quad (28)$$

α_m is the mirror loss where R_f is reflectivity of front facet; R_r is reflectivity of rear facet

α_{int} is the Internal loss; v_g is group speed inside the cavity.

γ_g is the carrier recombination rate that can be used to define the spontaneous carrier lifetime τ_g . Both radiative and non-radiative recombination processes contribute to γ_g .

$$\tau_g = (A_{nr} + BN + CN^2)^{-1} \quad (29)$$

A_{nr} is recombination rate due to mechanisms such as trap or surface recombination; B is the radiative recombination coefficient and C is related to Auger recombination process.

R_{sp} is spontaneous emitted photon intensity which is added to the intra-activity photon density and indispensable.

$$R_{sp} = \beta_{sp} \gamma_{sp} \tau_g N \quad (30)$$

β_{sp} is referred to as the spontaneous emission factor;

$$\gamma_{sp} = BN/\tau_g \quad (31)$$

$F_p(t)$ and $F_q(t)$ are noises from spontaneous emission process and $F_N(t)$ is the noise from carrier generation and recombination process. They are all incorporated by adding Langevin noises. In Langevin noise sources, they become

random and their dynamics are governed by the stochastic rate equations. When correlation time of the noise sources are much shorter than the relaxation times γ_s^{-1} and γ^{-1} (system has no memory). Under the Markovian assumption, the Langevin forces satisfy:

$$\langle F_i(t) \rangle = 0 \quad (32)$$

$$\langle F_i(t) F_j(t') \rangle = 2D_{ij} \delta(t - t') \quad (33)$$

where D_{ij} is the diffusion coefficient associated with the corresponding noise source. In a rigorous approach, D_{ij} can be explicitly expressed, by evaluating the second moment variables in equation (34) ~ (39) as:

$$D_{PP} = R_{sp} \bar{P} \quad (34)$$

$$D_{\phi\phi} = R_{sp}/4\bar{P} \quad (35)$$

$$D_{P\phi} = 0 \quad (36)$$

$$D_{NN} = R_{sp} \bar{P} + \gamma_s \bar{N} \quad (37)$$

$$D_{NP} = -R_{sp} \bar{P} \quad (38)$$

$$D_{N\phi} = 0 \quad (39)$$

\bar{P} and \bar{N} are steady-state average values of carrier and photon populations, respectively.

G is dynamic gain and N is dynamic carrier density. When G is simply linear dependent on N,

$$G(N) = \Gamma v_g a(N - N_0) \quad (40)$$

Here a is gain constant; N_0 is transparent (threshold) carrier density.

ith mode gain is given by:

$$G_i(f) = G_0 \left[1 - \left(\frac{f_i - f_0}{\sqrt{2}\Delta f_3} \right)^2 \right] \quad (41)$$

G_0 is maximum gain at f_0 and Δf_3 is the 3dB gain band width

$$f_i = f_0 + i\Delta f_{mode} \quad (42)$$

Δf_{mode} is mode spacing of laser

From equation (40), (41) and (42), we can get ith mode gain is

$$G_i(f) = G_0 \left[1 - \left(\frac{i\Delta f_{mode}}{\sqrt{2}\Delta f_3} \right)^2 \right] = \Gamma v_g a (N - N_0) \left[1 - \left(\frac{i\Delta f_{mode}}{\sqrt{2}\Delta f_3} \right)^2 \right] \quad (43)$$

2.2 Injection Locked Fabry-Perot Laser Diode

In the semiconductor lasers, it is practically impossible to satisfy simultaneously the requirements for high power output, spectral purity of the emitted radiation and economical. This leads to investigate the conception of injection locked in which two coupled lasers operate in conjunction. The first laser (Master Laser), operated in low power and low efficiency, emits a stable single mode output which is then injected into a comparatively high power laser (Slave Laser), quenches completely all the modes of this laser and forces the second laser working like a single mode laser with high power output (See.Fig.2-6) under the appropriate conditions of the frequency detuning and the injection

strength.

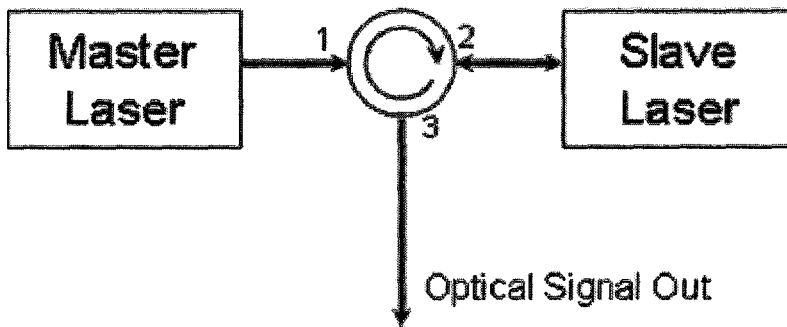


(Fig.2-6 Diagram of Injection Locked)

The characteristics of optical injection locked in semiconductor lasers originated from the fact that the line width enhancement factor has a non-zero definite value. As a viewpoint of laser dynamics, an optical injection from a different laser means the introduction of an extra degree of freedom to the laser. Therefore, various dynamics are observed by optical injection.

Injection locked F-P LD can be described by rate equation model (RE) or by Fabry-Perot model (F-P) which is often used in Fabry-Perot amplifier model.

F-P model is used to express the locking bandwidth in terms of the electric field. The electric field and carrier density have a range of injection-locked solutions that are strongly dependent upon the line width enhancement factor.

Equation (44)[9] describes the electric field after one round-trip where E_k is the field inside the cavity after the k-th round-trip, Δf is the round-trip phase detuning of the injected light with respect to the empty cavity, and R is the reflectance of the mirrors. E_{inj} is the injection light. N is the carrier density. It is

assumed for simplicity that both mirrors have the same reflection coefficient of \sqrt{R} [9].

$$E_{k+1} = R \exp((1 + j\alpha)N + i\Delta f) E_k + \sqrt{1-R} E_{in} \quad (44)$$

The steady-state field inside the cavity can be found by setting

$$E_{k+1} = E_k = E_s \quad (45)$$

Where E_s is steady-state carrier density

which results in:

$$|E_s|^2 = \frac{(1-R)|E_{in}|^2}{(1-R^2 \exp(2N)) - 2R \exp(N) \cos(\alpha N + \Delta f)} \quad (46)$$

Equation (47)[9] describes carrier density in a stability analysis of the F-P model:

$$N_{k+1} = P - \frac{N_k}{\tau_c} - N_k |E_k|^2 + N_k \quad (47)$$

$$N_{k+1} = N_k = N_s \quad (48)$$

The FP cavity allows for injection locking over the full range of detuning due to the influence of adjacent modes. Regions of this range of injection locking are dynamically unstable, so it is not advisable to exploit the continuous locking range in optical amplifier applications. Moreover, FP model does not consider the dynamic stability of injection locking.

Phenomenological RE model is commonly used to describe injection locked phenomenon in semiconductor including the carrier dependence of the refractive index [10].

In the injection locked situation, the RE model should be modified by

adding a term that includes the external injection. Optical injection locking is a coherent phenomenon, so that the discussion must be based on the complex electrical field instead of the photon number. Because $|E(t)|^2$ corresponding to the photon density P can be expressed as equation (22), E should be normalized [8].

In a master-slave injection locked F-P LD infrastructure, we assume detuning $\Delta f = |f_M - f_S|$ is very small; photon number P_M of master laser is small comparing to the photon number P_S of slave laser.

We only consider of the RE model of slave laser with (22) ~ (26), we can get [8]:

$$\frac{dE_0}{dt} = \frac{1}{2} (1 + j\alpha)(G_0 - \gamma)E_0(t) + F_0^s(t) + k_0 E_{inj}(t) \exp(-j2\pi\Delta f t) \quad (49)$$

$$\frac{dE_1}{dt} = \frac{1}{2} (1 + j\alpha)(G_1 - \gamma)E_1(t) + F_1^s(t) \quad (50)$$

$$\frac{dN}{dt} = \frac{I}{eV} - \gamma_r N - \sum_i G_i |E_i|^2 + F_N(t) \quad (51)$$

Noised rate equation formulations consider multi-longitudinal mode, spontaneous emitting noise, a detuning frequency offset Δf and $E_{inj}(t)$ which works as master laser in injection locked infrastructure.

Equation (49) expresses the governing field equation of the time change of the electric field in the LD cavity longitudinal mode with the external light injected which is the third item of the equation. E_0 is the complex amplitude of the 0th mode of electrical field; G_0 is gain of 0th mode; γ is the loss of the cavity;

$F_E^0(t)$ is the spontaneous emission noise coupled into the 0th mode; E_{inj} is complex amplitude of external light injected into 0th mode. k_e is coupling efficiency[11][12]:

$$k_e = \frac{\gamma_0(1-R_f)}{2L\sqrt{R_f}} \sqrt{\frac{\eta(\sqrt{R_f} + \sqrt{R_D})(1 - \sqrt{R_f}\sqrt{R_D})}{\sqrt{R_D}(1 - \sqrt{R_f}) \ln\left(\frac{1}{R_f R_D}\right)}} \quad (52)$$

Equation (50) expresses the i th mode electrical field with respect of the time change. G_i is gain of i th mode; $F_E^i(t)$ is the spontaneous emission noise coupled into the i th mode.

The time change of carrier density inside the active region interaction with the laser radiation is described in equation (51).

In the formulations, a is gain constant; N_0 is transparent (threshold) carrier density; Δf_g is 3dB gain Bandwidth; Δf_{mode} is mode spacing of F-P LD.

Both F-P model and RE model give identical results in the limiting case of no injected signal. The difference increases with the increase of the injected signal level. F-P model and the RE model give the same results for low laser optical injection powers. But at higher injection powers, F-P model predicts a wider locking bandwidth so is more useful for large signal. RE model is suitable for small signal applications to study the dynamic characteristics and modulation properties of injection locked semiconductor lasers. Since a modulated injection locked F-P LD is needed in a wavelength independence ONU [8] [9] [10], RE

model will be studied here.

Now we are going to study the dynamic characteristics associated with FTTH network only with RE model. FTTH transmitter needs a high and pure output with broadband modulation and broadband gain spectral width and lower noise:

1) Spectra:

Experiments from [13] demonstrates that with the injection of a single mode coherent light, oscillation occurs first at the injected mode by triggering of the injected light. Fig.2-6[13] shows the spectra of AlGaAs heterostructure laser modeulated by 500Mbit/s. The left side picture is got without injection and the right side picture is got with injection of -28.5 dBm. At the same time, the gains of the side modes are suppressed further. Fig.2-7[13] shows the relation between injected power and lasing mode and side modes. While the injected power increases, the lasing mode power consistently increases and side modes powers consistently decrease. The locking range is widened as the drive current decreases [13].

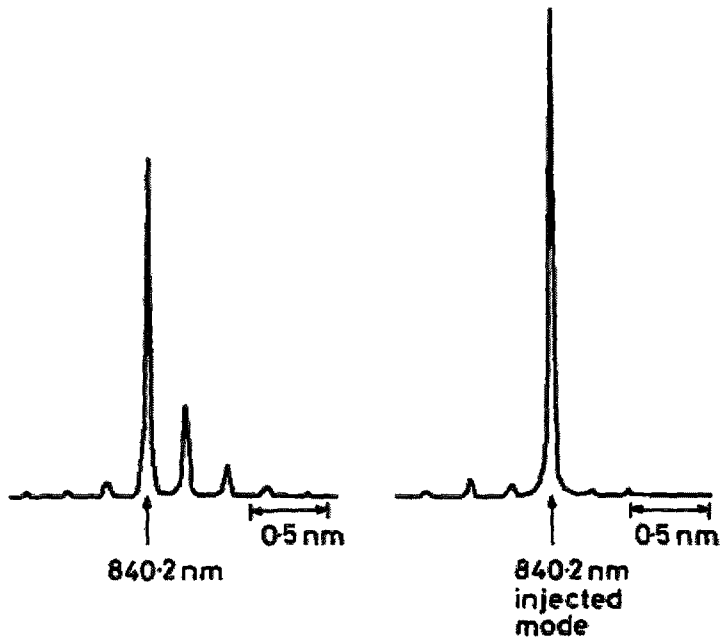


Fig.2-7 spectra of AlGaAs heterostructure laser modulated by 500Mbit/s

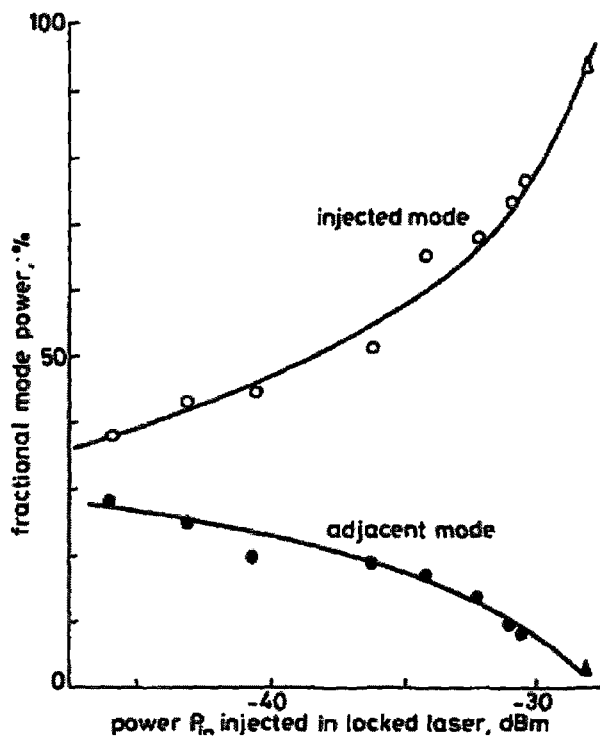


Fig.2-8 power ratio between injected mode and lasing mode and side modes.

2) Locking range

In laser cavity, relaxation oscillations are caused by an intrinsic resonance in the gain saturation process and by the subsequent coupled fluctuations of light intensity and carrier density [14]. The optical injection induces a modulation in the free-running signal before the locking occurs for detuning under the lower limit of the locking range. When the locking occurs, the operation point is moved through the locking range. Only in this case, Injection locked F-P LD outputs stable high power longitudinal single mode. At the upper limit of the stable locking range, the locked laser becomes unstable, i.e. the laser becomes multimode [14].

Width of locking range is strongly dependent on the phase amplitude coupling [14]. Spectral hole burning and lateral carrier diffusion, treated analytically by a gain saturation term, increases width of locking range [14].

Locking range can be expressed by detuning. [15] shows that the stable locking range can be increased significantly by the nonlinear gain by about an order of magnitude.

[9] reports that the line width enhancement factor influences the injection locked states; the lower carrier injection locked states are dynamically stable; large external injection powers states allow for

injection locking over the full range of detuning, some part of the range is dynamically unstable, even when line width enhancement factor is zero.

We use RE model to solve stable locking range problem [7]:

In a master-slave injection locked F-P LD infrastructure, detuning $\Delta f = |f_M - f_S|$ is very small; photon number P_M of master laser is small comparing to the photon number P_S of slave laser. Complex electrical field of the master laser and slave laser are:

$$E_M = \sqrt{P_M} \exp(-i\phi_M(t)) \quad (53)$$

$$E_S = \sqrt{P_S} \exp(-i\phi_S(t)) \quad (54)$$

The phases ϕ_M and ϕ_S are generally time dependent functions, but the master laser is under steady-state operation and its phase is assumed to be $\phi_M = 0$. Though the phase of the slave laser fluctuates with time, it is approximated as a small fluctuation and assumed to be a constant value in the following. Taking these assumptions into consideration, the rate equation of the slave laser can be expressed as [7]:

$$\frac{dE_S(t)}{dt} = \frac{1}{2}(1 - i\alpha)G_N \{n(t) - n_{th}\}E_S(t) + \frac{K_{inj}}{\tau_{in}} E_M(t) \exp(i2\pi\Delta f t) \quad (55)$$

where respectively, K_{inj} is the injection coefficient, and τ_{in} is the round trip time of light in the laser cavity.

Then we can get the stable locking range should be[7]:

$$\Delta f < \frac{\sqrt{1+\alpha^2}}{\tau_{in}} \sqrt{\frac{P_S}{P_M}} \quad (56)$$

Fig.2-9 shows the areas of optical injection locking in the phase space for the frequency detuning between the master and slave lasers and the injection ratio. The solid curves show the boundaries between optical injection locking and non-locking regions. Within the region of the optical injection locking, there are stable and unstable locking areas. The boundary of the unstable and stable injection locking areas is denoted by a dotted curve. The asymmetric feature of stable injection locking again originated from the fact that the α parameter has a non-zero value in semiconductor lasers [7].

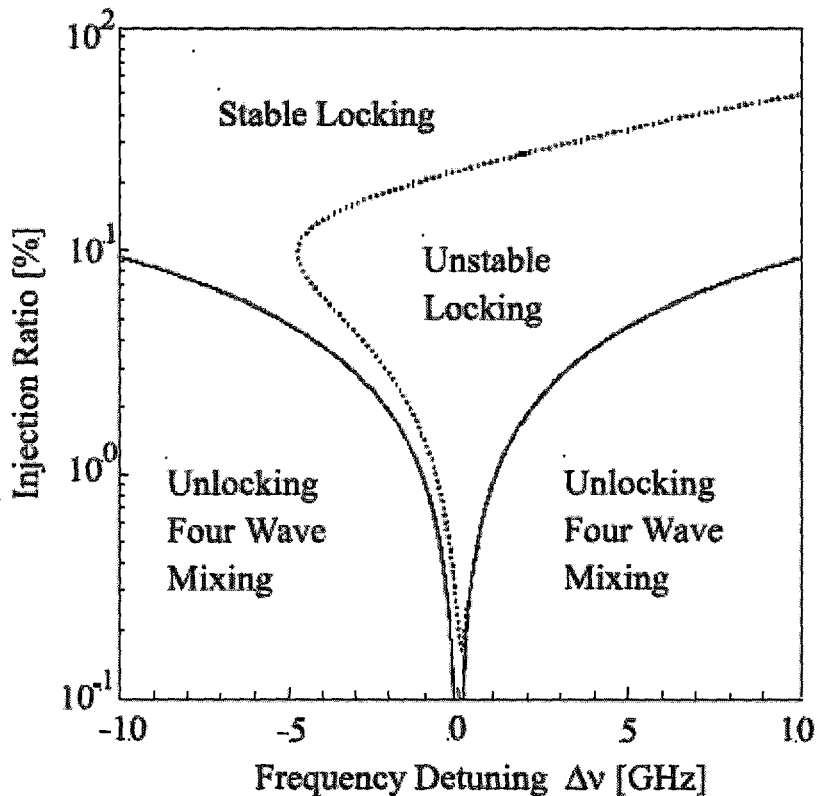


(Fig.2-9 Locking and unlocking regions in phase space of frequency

detuning and injection field)

3) Gain

Fig. 2-10 [16] shows a dynamic process of the relaxation oscillation of LD in the temporal evolution. Photon population in all modes remains zero for a time period known as the turn-on delay time after which it increases rapidly. Relaxation oscillation takes several nanoseconds to become sufficiently damped for mode intensities to reach their steady-state values.

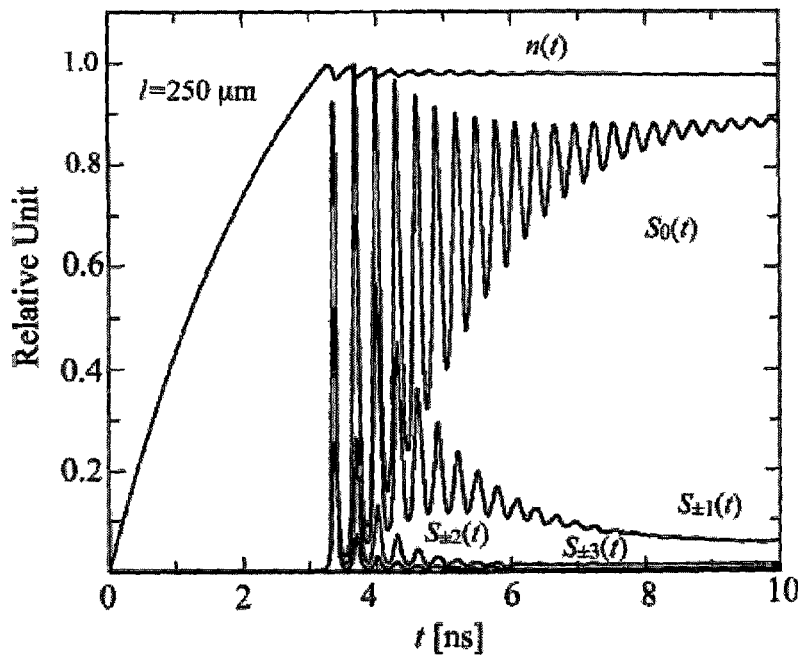


(Fig.2-10 time evolution of carrier density and photon population under relaxation oscillations)

Equation (57) gives the gain of the medium at the threshold and its relation through the carrier density n_0 at the transparency using Taylor

series up to the first order.

$$g_m = \frac{\partial g}{\partial n} (n_m - n_0) \quad (57)$$

When LD oscillates well above the threshold, the effect of gain saturation must be taken into account [16] as equation (58)

$$g = \frac{g_m}{1 - \epsilon |E|^2} \quad (58)$$

When the saturation effects is very small (as often the case), we can approximate the gain as equation (10)

$$g \approx g_m (1 - \epsilon |E|^2) \quad (59)$$

Physically in semiconductor laser, the gain spectrum is asymmetric with respect to the gain spectrum peak and as a consequence, the associated refractive index near the gain peak varies appreciably with the excited carrier density which causes gain nonlinearity. The resulting gain compression coefficient ϵ is found to be proportional to the frequency derivative of the differential refractive index at the lasing frequency (see equation (59)).

4) Modulation bandwidth

The modulation bandwidth of a semiconductor laser at free running state is limited by the relaxation oscillation frequency. However, when a semiconductor laser is strongly injected under stable injection locking conditions, the modulation bandwidth of the slave laser is greatly enhanced. At the same time, the suppression of laser noises is achieved,

but the strong modulation gives rise to frequency chirping in the laser oscillation [17].

5) Noise

As analyzed before, RIN comes mainly from spontaneous emission noise which is considered as a white noise process with a Gaussian probability distribution. In injection locked situation, master laser injects a single mode light into slave laser and injects its spontaneous emission noise as well. According to Lang [18], carrier density in the active region decreases with light injection yielding an increasing refractive index, resulting in a decreasing cavity resonance frequency of the slave laser. So the locking can be achieved only if the injected light frequency approximately coincides with the resonance frequency which is downshifted by light injection.

[19] demonstrates the relation among detuning, line width enhancement factor, injection power and RIN numerically considering spontaneous emission noise and other noises by solving rate equations. When line width enhancement factor is large, RIN of slave laser is always larger than RIN of free running slave laser [19]. While line width enhancement factor is small, part of its RIN is smaller than free running status. In Fig.2-13 RIN in the frequency range -3.0GHz ~ -.175GHz is smaller than free running status [19]. Here line width enhancement factor is 3. With the condition of the same line width enhance factor, larger input

signal decreases the frequency range in which RIN of injection locked slave laser is smaller than its free running status.

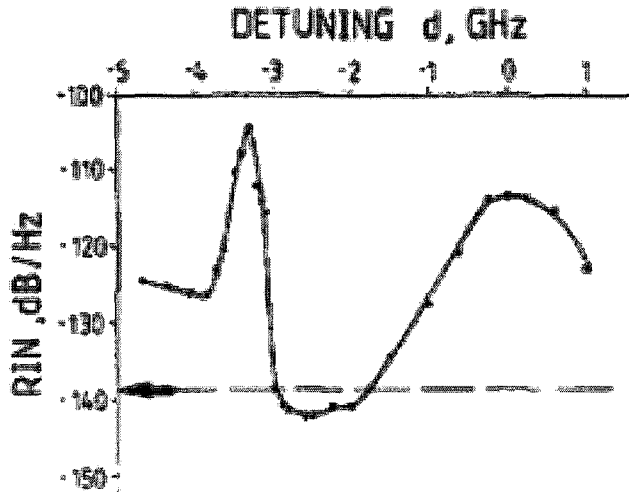


(Fig.2-11 relation between RIN and detuning when line width enhancement factor is small)

2.3 Summary

Free running F-P LD exhibits characteristics of multimode oscillation. It oscillates in a single longitudinal mode with a high output after injected by a weak coherent optical signal whose wavelength and injected power are within its stable locking range.

F-P model and the RE model give the same results for low laser optical injection powers. But at higher injection powers, F-P model predicts a wider

locking bandwidth so is more useful for large signal. RE model is suitable for small signal applications to study the dynamic characteristics and modulation properties of injection locked semiconductor lasers. Since a modulated injection locked F-P LD is needed in wavelength independence ONU.

We setup theoretical model for both free running F-P LD and injection locked slave laser. We analyzes specific characteristics of injection locked F-P LD based on RE model. RE model can explain experiments well.

Chapter3. Narrow Band Amplified Spontaneous Emission

3.1 Spectrum sliced ASE

In the injection locked F-P LD architecture, a master laser which emits a weak coherent longitudinal single mode light is necessary. But in WDM-PON architecture, it's price prohibitive to supply each ONU one wavelength coherent signal. However, a reflective architecture is considered in which all of the individual wavelengths are provided by a shared network resource (See Fig.1-4).

Moreover, some experiments demonstrate that the F-P LD injected by a sliced broadband light source can emit much better longitudinal single mode signal[20][21] which supports the fundamental about WDM-PON reflective architecture (see Fig.3-1[3]).

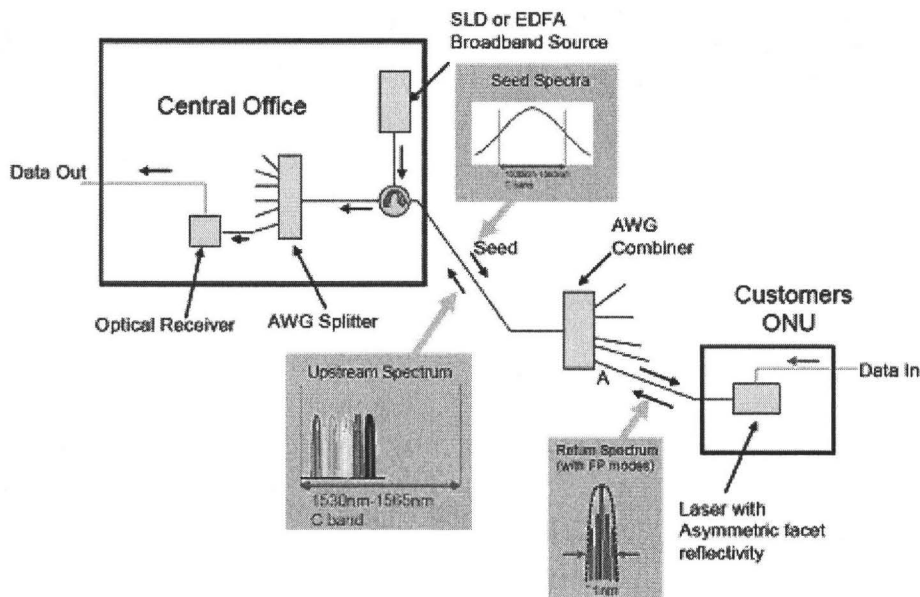


(Fig.3-1 F-P LD injected locked by sliced ASE in the reflective architecture in WDM-PON)

In the reflective architecture, a seek broadband light source in the central office is transmitted to the remote node (RN), sliced by a filter (such as a AWG) then injected into a F-P LD which is identical in every ONU, modulated directly by user band width then transmitted back to the central office through the same AWG. In this architecture, the sliced broad band optical signal functions as the master laser and the identical F-P LD functions as the slave laser.

A broadband light source (BLS) is needed in the central office to act as a seed light for remote ONUs. BLS can be a light-emitting diode (LED), a super luminescent diode (SLD) or an amplified spontaneous emission (ASE) based on erbium-doped fiber amplifier (EDFA).

LED and SLD can be fabricated at a low cost and modulated directly.

However, their output power is not sufficient enough, normally lower than -10 dBm. They cannot accommodate many ONUs after being spectrum sliced.

ASE based on EDFA technology can improve the output power by increasing the pumping power. An associated lab has been reported by using commercially available erbium-doped fiber, the broadband light source with two output ports was produced. One supplies C-band ASE light with 20.5dBm output total power and another supplies L-band ASE light with 15.7dBm [22].

Broadband ASE signal is a complex Gaussian process. The amplitude of it follows the Gaussian distribution and its mean value is zero as equation (60). Its phase is uniformly distributed from 2 to 2π [23] [24].

$$\langle E_{ASE}(t) \rangle = 0 \quad (60)$$

$$\langle E_{ASE}(t) E_{ASE}^*(t - \tau) \rangle = P_s \delta(\tau) \quad (61)$$

In equation (61), δ is Kronecker's delta function and angle brackets denotes ensemble average. P_s is the power spectral density of ASE light [23] [24].

ASE transforms to be narrow band ASE (NASE) by equation (62). $H(f)$ is the transferring function of the spectrum slicing filter which determines the spectral shape of the spectrum sliced ASE.

$$E_{NASE}(t) = F^{-1}\{F[E_{ASE}(t)]H(f)\} \quad (62)$$

After sliced by band pass filter, ASE is still complex Gaussian process. But it is not white anymore since it passes a linear filter. Moreover, the sliced ASE is not coherent. So it is difficult to have a precise solution for direct

understanding of injection locked F-P LD due to statistical property of the injected narrow band ASE [24]. Since all the analysis which has been demonstrated by calculations are based on a coherent injection.

3.2 Summery

Experiments have demonstrated that a spectrum sliced ASE can work similar to a coherent injected optical signal to force F-P LD output longitudinal single mode signal. But sliced ASE single is not a coherent signal. So it is difficult to have a precise solution for direct understanding of injection locked F-P LD due to statistical property of the injected this kind of narrow band ASE. A theoretical way should be found out to explain the experiments. We will answer this question later by solving the RE model.

Chapter4. Experiments for Injection Locked F-P LD with NASE

4.1 Introduction

Un-cooled, un-isolated F-P LD which is less expensive than LED and typically has over ten times the output power than LED is so far one of the best choices to supply a colorless ONU. However, a F-P LD has its own shortcomings when used under external injection locked in the access network where lasers have to satisfy the fiber-to-the-home working environments.

First F-P LD should work well in temperature arrangement from -20°C ~ 60°C which is the working temperature standard of FTTH. Considering temperature rise in the package, the laser diode chip should be operable in the temperature range of 20°C ~ 75°C at least. Since the working environment cannot guarantee a stable working temperature, the wavelengths of the lasing modes will vary with time; therefore the mode spacing of the F-P LD should be larger than the channel spacing of the filter which is used to slice the broadband light source. This just ensures that only one lasing mode can spectrally overlap with the injected narrow band ASE considering the wavelength change due to temperature.

The second shortcoming is that a F-P LD does not inherently have a broad optical spectrum (see Fig.2-3-c). However, experiments demonstrate that

asymmetric multiple quantum-well (AMQW) F-P LD structure has a wide band gain spectrum. In AMQW laser each MQW is in a single active region with each well designed to operate on different transition energy [29][30][31].

The last and the most impact drawback while using injection locked F-P LD is the high relative intensity noise (RIN). Injecting ASE signal into F-P LD through a narrow optical band-pass filter will convert mode-fluctuations into RIN [19] [28]. The narrower the optical filter is, the higher the RIN will feed in F-P LD [20].

4.2 Experiments

We talk about one experiment mainly based on [20] [21].

Fig.3-1 is the diagram about the experiment setup

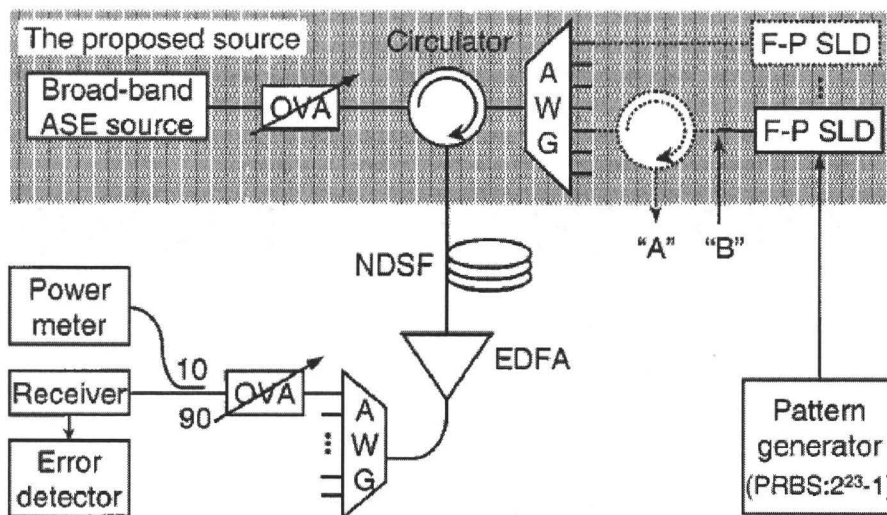


(Fig.4-1 diagram about experiment setup)

In the experiment, the broadband ASE is a two stage EDFA pumped counter-directionally with laser diodes at 1480nm.

An optical variable attenuator (OVA) is used to control the ASE power injected into the F-P LD.

An optical circulator with an insertion loss of 0.7 dB separates the injected broad-band ASE and the output of the F-P LD.

The broadband ASE signal in the central office is sliced by the AWG (the one in the shadow in the Pic.4-1) which functions as a de-multiplexer and linear filter with 0.24 nm band width. Then the sliced narrow band ASE signal is injected into an identical F-P LD, modulated by a 155MHz user band width generated by Pattern Generator (PRBS:2²³-1) then is transmitted back as an upstream signal.

The upstream signal is multiplexed by the same AWG and is transmitted through a 20kms Non-dispersion Single mode Fibre (NDSF). In the central office, the upstream signals are de-multiplexed by another AWG with 0.32 nm band width and are sent to the power meter and error detector in order to detect the transmitting performance.

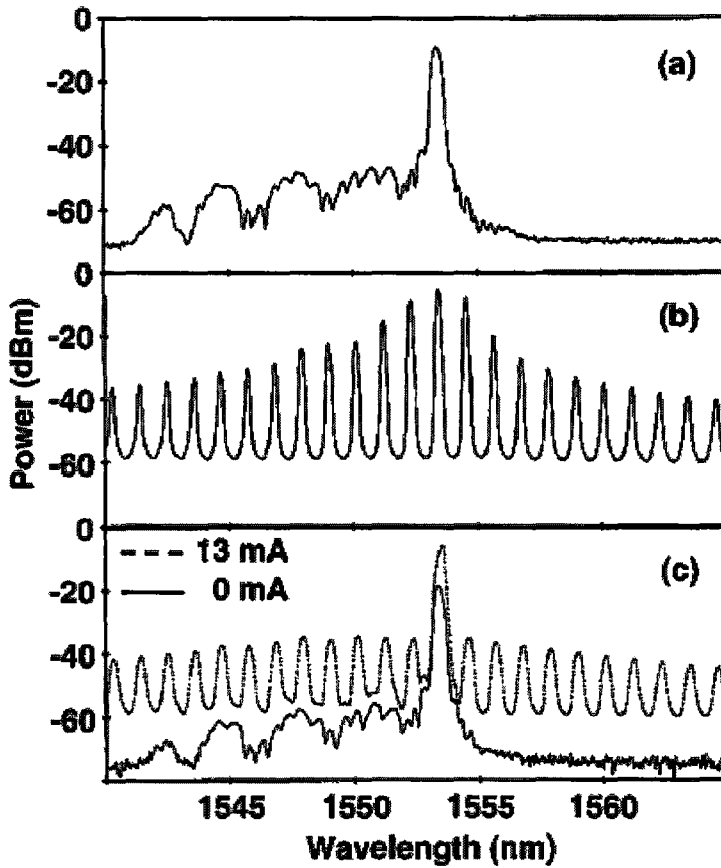
The experimental setup agrees with the WDM-PON reflective architecture.

Fig.3-2[21] shows measured spectrum of ASE injected F-P LD: (a) is the spectrum of narrow band ASE injecting light signal; (b) is the spectrum of free running F-P LD; (c) is the spectrum of F-P LD after injection locked by narrow band ASE.

The measured output power at point A and point B shown in Fig.3-1 is as below:

	A	B
Narrow band ASE		-6dBm
Free running F-P LD	-2.5dBm	
Injection locked F- P LD	-2.6dBm	

(Table 4-1 light powers at reference points)



(Fig.4-2 measured spectrum of ASE injected F-P LD (1))

The bias current is 13mA; The wavelength at the peak power is 1553.33nm. Roughly observing Fig.4-2 and referring Table 3-1, we can get the following results about F-P LD that Side Mode Suppress Rate in free running status is less than 2.4dB and Side Mode Suppress Rate in injection locked status is more than 29dB.

In the central office the error detector shows that error is zero.

In the experiment the wavelength at peak output power is changed by

changing the temperature of AWG. The injection locked F-P LD maintains the locking status when the peak of the wavelength changes within $\pm 130\text{GHz}$. Another experiment [20] shows the similar results in the similar network architecture. The differences are: the transmitting distance is 10kms; the user band width is 1.25GHz; the bias current is 20mA; the input power before fiber pigtail is 1.8dBm; the central wavelength is 1555.06 nm which is similar to the first experiment. The transmitting is error free. Fig.3-3 [20] is its spectra output.

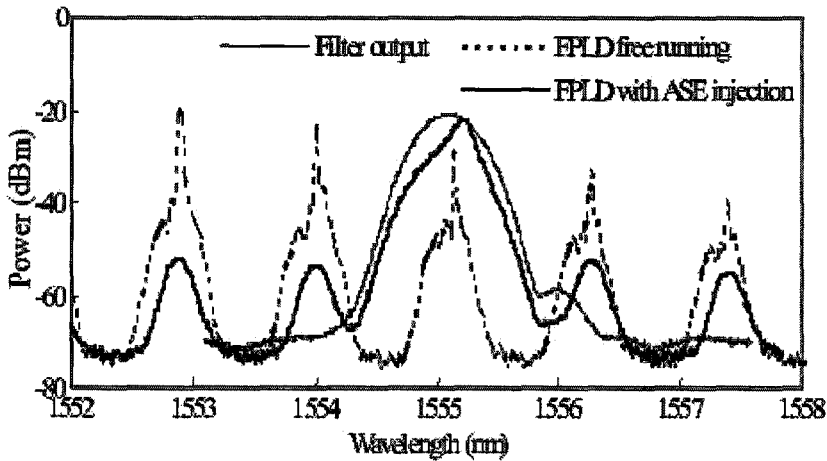


(Fig.4-3 Measured spectrum of ASE injected F-P LD (2))

In the Pic.4-3, the SMSR in the locked status at peak is more than 40dB; the SMSR in the free running status is about 2 dB which is similar with the first experiment.

Chapter5. Simulations for Injection Locked F-P LD with NASE

5.1 Introduction

In the injection locked F-P LD architecture, the slave LD is an identical F-P LD and the master LD is the narrow band ASE Gaussian Complex noise which is not coherent. Moreover, a solitary laser is a second-order system but an injection locked laser is a third-order system [15].

RE model is studied here since it is suitable for small signal applications to study the dynamic characteristics and modulation properties of injection locked semiconductor lasers. Here we discuss its complex field instead of the photon number.

When consider the RM model numerically, we assume the following:

- (1) Nonlinear gain is considered by considering gain compression factor
- (2) The cavity losses are uniformly distributed along the laser cavity;
- (3) The guide transverse dimension is small enough to allow single mode longitudinal operation;
- (4) The spatial gain variation along the cavity is neglected
- (5) Spontaneous emission noise is considered while mode partition noise is ignored even in direct modulation since a strong spontaneous emission is

coupled to a particular mode [21]

According to (5), in equation (51) $F_N(t)$ is ignored.

According to (1), gain compression factor should be considered. From equation (43) and (59), we can get:

$$G_i = \frac{\Gamma \nu_g a(N-N_0) \cdot \left[1 - \left(\frac{2\Delta f_{\text{noise}}}{\sqrt{2}\Delta f} \right)^2 \right]}{[1 - \epsilon \sum |E_i|^2]} \quad (63)$$

G_i is approximately a Lorentzian function

Then equation (49), (50) and (51) can be expressed as

$$\frac{dE_0}{dt} = \frac{1}{2} (1 + j\alpha)(G_0 - \gamma)E_0(t) + F_E^0(t) + k_s E_{\text{noise}}(t) \exp(j2\pi\Delta f) \quad (64)$$

$$\frac{dE_i}{dt} = \frac{1}{2} (1 + j\alpha)(G_i - \gamma)E_i(t) + F_E^i(t) \quad (65)$$

$$\frac{dN}{dt} = \frac{J}{qV} - \gamma_s N - \sum_i G_i |E_i|^2 \quad (66)$$

In equation (64), because gain compression factor is always negative in semiconductor laser, we use $\epsilon \approx \epsilon_{\text{sc}}(1 + \epsilon|E|^2)$ instead of equation (59) where ϵ is the gain compression factor. We use $\exp(j2\pi\Delta f)$ instead of $\exp(-j2\pi\Delta f)$ at the same time.

Equation (64) ~ (66) are the extended version of an injection locked semiconductor laser diode to coherent injection light [8][12].

Noised rate equation formulations consider multi-longitudinal mode, spontaneous emitting noise, nonlinear gain fluctuation with respect to all noise linked to gain

compression factor, a detuning frequency offset Δf and external narrow band ASE noise which works as master laser in injection locked infrastructure.

$F_E^0(\omega)$ is the spontaneous emission noise coupled into the 0th mode; $F_E^i(\omega)$ is the spontaneous emission noise coupled into the i th mode. Both of them agree with equation (32) ~ (39).

E_0 is the complex amplitude of the 0th mode (lasing mode) of electrical field; G_0 is gain of 0th mode; Δf is the frequency of detuning between sliced ASE and the laser mode at free-running state.

Equation (65) expresses the i th mode electrical field with respect of the time change. G_i is gain of i th mode.

The time change of carrier density inside the active region interacting with the laser radiation is described in equation (66).

L : cavity length; η : coupling efficiency between the pigtail fiber and the active region

R_f : reflectivity of front facet; R_r :reflectivity of rear facet

A_{nr} : nonradioactive recombination coefficient; B :radioactive recombination coefficient

C : auger recombination coefficient; α_{int} : internal loss

α_m : mirror loss; γ_s : carrier recombination rate

f_{ASE} : the centre frequency of sliced ASE; f_0^m :frequency of 0th mode at threshold

The optical power of the i th mode P_i is expressed as below [23] [24]

$$P_i = \eta h f_i v_g \alpha_m \frac{\Gamma}{\Gamma} |E_i(t)|^2 \cdot \left[\frac{\sqrt{R_B}(1-R_F)}{(\sqrt{R_F} + \sqrt{R_B})(1 - \sqrt{R_F}\sqrt{R_B})} \right] \quad (67)$$

h : Planck constant; f_i : i th mode frequency; η : coupling efficiency between the pigtail fiber and the active region.

$E_{NASE}(t)$ is the narrow band ASE noise which is coupled into lasing mode of F-P LD which agrees with equation (60) ~ (62). The power of ASE which is coupled into F-P LD can be measured. Then we can get $E_{NASE}(t)$ by

$$|E_{NASE}(t)|^2 = \frac{P_{NASE}\Gamma}{2h\eta v_g w d} \quad (68)$$

w : width of the active region of LD; d : depth of the active region of LD.

The theoretical model of injection locked F-P LD is solved numerically by fourth-order Runge-Kutta method.

λ	Wavelength at gain peak	$1545 \times 10^{-9} \text{m}$
L	Cavity length	$600 \times 10^{-6} \text{m}$
w	Width of active region	$15 \times 10^{-6} \text{m}$
d	Depth of active region	$0.2 \times 10^{-6} \text{m}$
Γ	Confinement factor	0.5
n_g	group index	3.5
α	Line width enhancement factor	3

β_{sp}	Spontaneous emission factor	$4 * 10^{-5}$
α_{int}	Internal loss	$1 * 10^8 m^{-1}$
R_f	Reflectivity of the front facet	0.01
R_b	Reflectivity of the rear facet	0.3
a	Gain constant	$2 * 10^{-20} m^2$
N_0	Transparent carrier density	$1 * 10^{24} m^{-3}$
A_{nr}	Non-radiative recombination coefficient	$1 * 10^9 s^{-1}$
B	Radiative recombination coefficient	$2 * 10^{-16} m^3 s^{-1}$
C	Auger recombination coefficient	$4 * 10^{-41} m^3 s^{-1}$
ϵ	Gain compression factor	$3.6 * 10^{-22} m^3$
η	Coupling efficiency between the pigtail fiber and the active region	0.4
Δf_g	3dB gain bandwidth	$5.0 * 10^{14} Hz$
Δf_{mode}	Mode spacing of F-P LD	$71.4 * 10^6 Hz$

(Table.5-1 Physical parameters of F-P LD)

Parameters are chosen mainly from the basic characteristics about injection locked F-P LD and others are referred by successful experiments [20]

[21] [23] [24]. (see table.5-1)

Central wavelength of 1545 nm which is in the C band guarantees the lower optical fiber attenuation and dispersion.

3dB band width of filter is $31.3 * 10^9$ Hz which is less than Δf_{mode} which is mode spacing of F-P LD.

The calculated threshold current is 22.5mA. The bias current of the F-P LD is 1.2 times of threshold current.

The time interval is 1ps and the simulation is extended to 100ns so that the frequency resolution is 10 MHz.

The detuning Δf is zero in order to simplify the simulation.

The number of mode of the F-P LD is five.

The broadband ASE and spontaneous emission noise are complex Gaussian process. They are both generated by random number generator in the simulation.

Then the narrow band ASE is calculated by equation (62).

5.2 Simulation results:

Free running F-P LD shows multimode characteristic longitudinally.

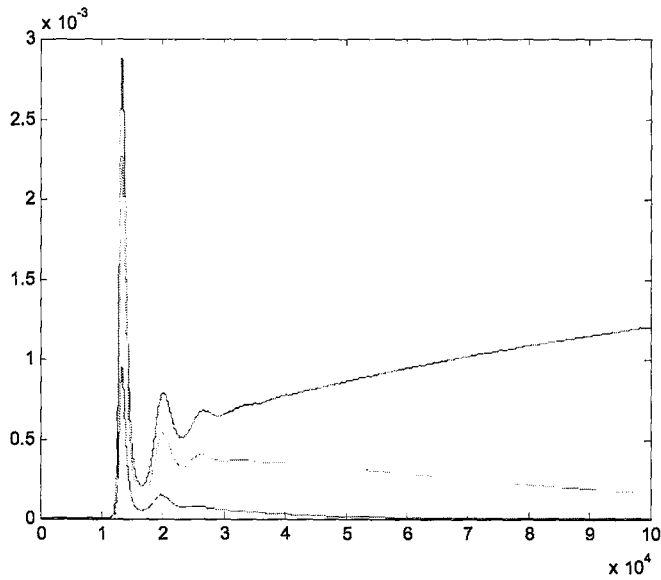


(Fig.5-1 Power output distribution in the free running F-P LD)

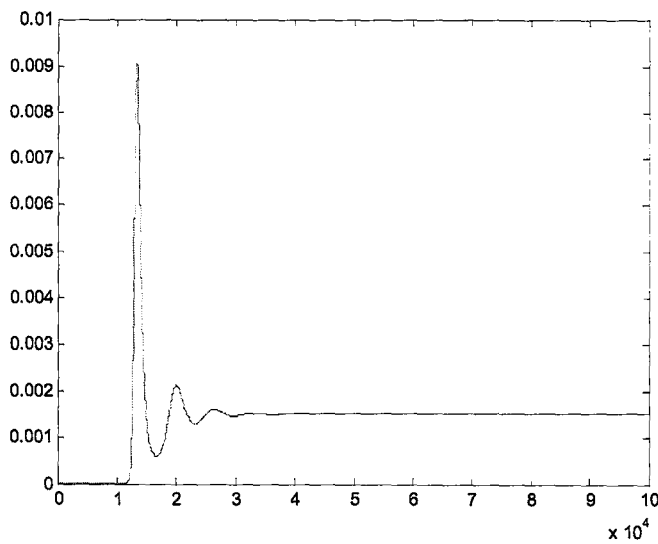


(Fig.5-2 Total power output distribution in the free running F-P LD)

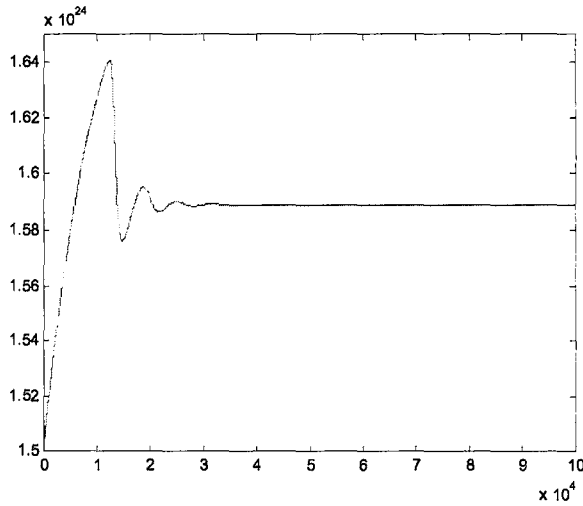


(Fig.5-3 Carrier density in free running F-P LD)

In Fig.5-1, the upper line expresses 0-th mode which is the main mode; the medium line expresses the 1-st mode and the lower line expresses the 2-ed mode. The power distribution is reasonable since the power of each mode is not supposed to be identical since the gain dispersion is included in the model.

Carrier density in the Fig.5-3 agrees with the result in Fig.2-10.

Then we use this model to analyze the following characteristics of F-P LD:

- (1) Power distribution of five modes in the cavity:

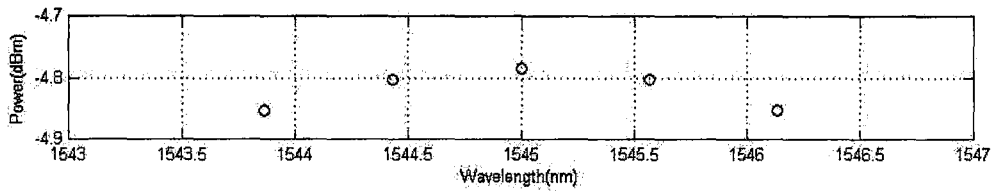


(Fig. 5-4 Power distributions in the free running F-P LD)

In Fig.5-4, the free running F-P LD also shows its longitudinal multimode characteristic. The side mode suppression ratio (SMSR) is about 0.02dBm.

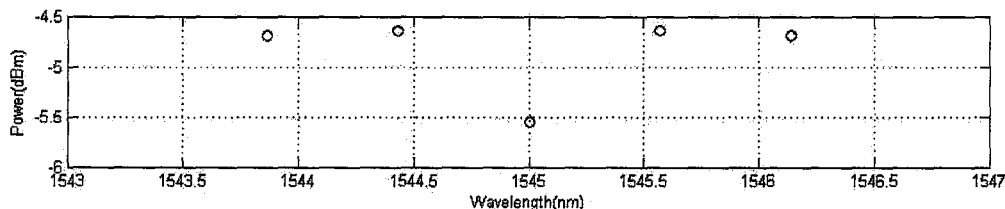


(Fig.5-5 Power distributions in the injection locked F-P LD with -50dBm ASE injection)

In Fig.5-5, F-P LD is injected by a very small sliced ASE signal. Since we assume that the detuning between sliced ASE and free-running F-P LD is zero, F-P LD shows four-wave and multi-wave mixing associated with the unlocked slave laser frequency and has a side peak in the spectrum due to regenerative amplification [7].

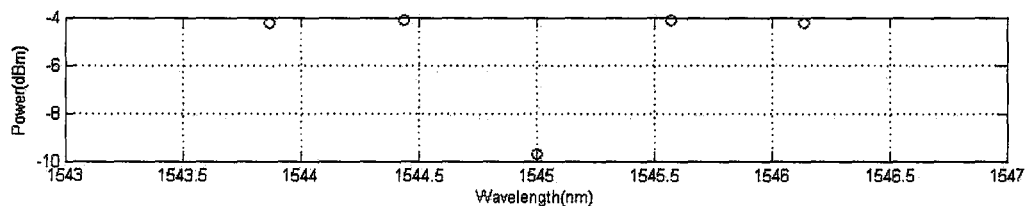


(Fig. 5-6 Power distributions in the injection locked F-P LD with -35dBm ASE injection)

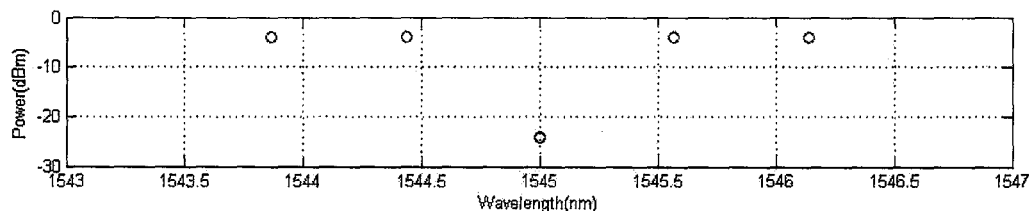


(Fig. 5-7 Power distributions in the unlocked F-P LD with -18.8dBm ASE injection)

In Fig. 5-6 and Fig.5-7, F-P LD is continuously unlocked.

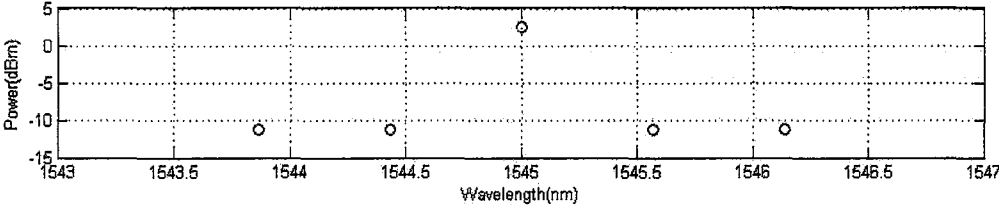


(Fig. 5-8 Power distributions in the injection locked F-P LD with -18.5dBm ASE injection)

However, after just added only 0.3 dBm more injection power, F-P LD reach out its threshold and starts to show its stable longitudinal single mode characteristic with the SMSR of 17dB.

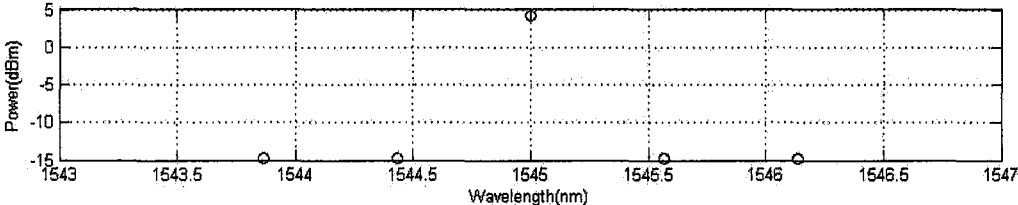


(Fig.5-9 Power distributions in the injection locked F-P LD with -10dBm ASE injection)

When the master laser power input reaches -10dBm, the injection locked F-P LD shows more longitudinal single mode characteristic with SMSR of 25dB

and its own output power of 4.9 dBm. SMSR of 25 dB is sufficient enough for DWDM-PON and the 4.9 dBm is good enough being as a transmitter in the optical single mode communication system. So we can get the conclusion that injection power of approximate -10dBm is the optimal injection power in this model. This result agrees with the lab result in Fig.4-2.

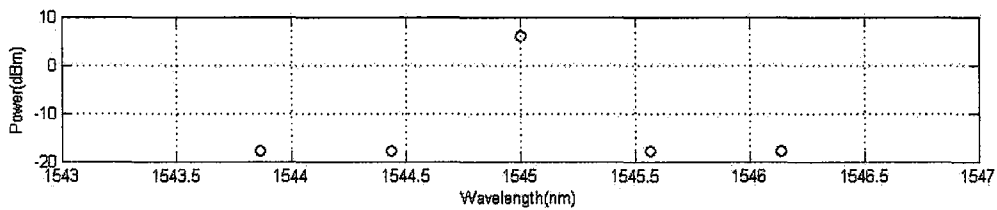


(Fig. 5-10 Power distributions in the injection locked F-P LD with -3dBm ASE injection)

SMSR and output signal of injection locked F-P LD consistently go up with the consistent master laser power going up. But the growing up ratio becomes slow gradually.

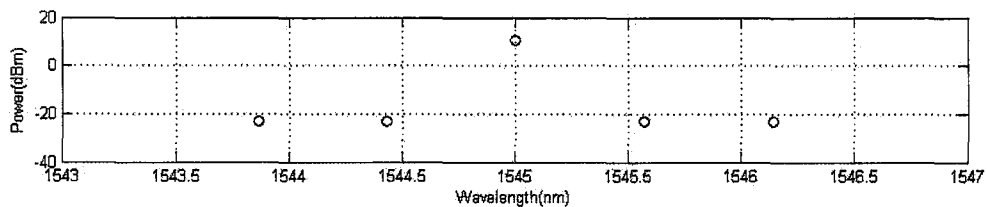


(Fig. 5-11 Power in the injection locked F-P LD with 10dBm ASE injection)

When a 10 dBm big ASE signal injects into F-P LD, the characteristics of F-P LD cannot be explained precisely by RE model anymore. In this case, the FP model can give more precise explanation in this case.

The simulation results about the power agree with Fig.2-7 and Fig.2-8.

(2) RIN

We calculated the RIN by assuming the receiver bandwidth is 1M which is referred by [6].

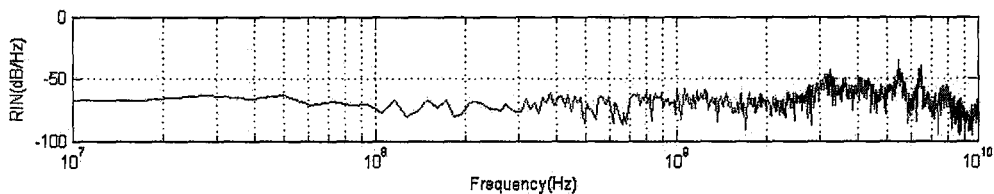


(Fig. 5-12 RIN in the free running F-P LD)

In Fig.5-12, RIN starts its high frequency peak in the relaxation oscillation of F-P LD at around 2.2 GHz.

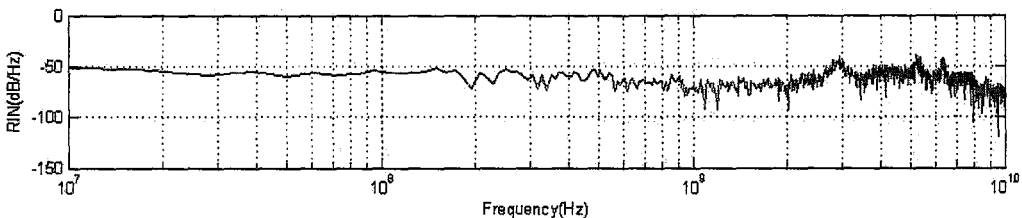


(Fig. 5-13 RIN in the injection locked F-P LD with -50dBm ASE injection)

Fig.5-13, the high frequency peak downshifts. The reason is that F-P LD is in the four-wave and multi-wave mixing associated with the unlocked slave laser

frequency. The relaxation oscillation frequency downshifts in this case. RIN even gets worse comparing to RIN in its free running status. The reason is the mode partition noise and mode hopping noise increase.

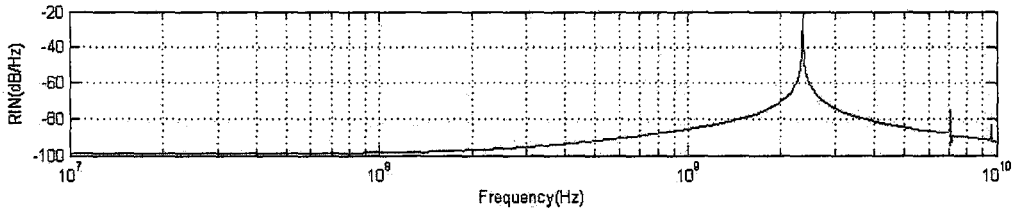


(Fig. 5-14 RIN in the injection locked F-P LD with -35dBm ASE injection)

In Fig.5-14, the relaxation frequency continuously downshifts but the light output gets more stable. However, the RIN gets better than RIN in its free running status in this case.

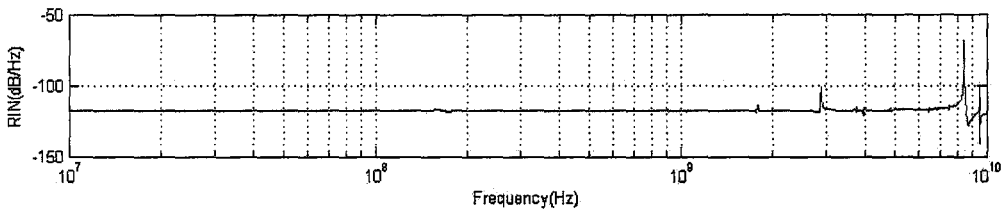


(Fig. 5-15 RIN in the injection locked F-P LD with -18.8dBm ASE injection)

In Fig.5-15, F-P LD runs around the nearby of stable locked area but F-P LD keeps staying in the four-wave and multi-wave mixing associated with the unlocked slave laser frequency status.

From now on, F-P LD reaches its injection locked status. F-P LD starts to output longitudinal single mode signal. RIN of the main mode almost equals to

that of the total mode (See Fig.5-16). Mode partition noise and mode hopping noise are extremely suppressed.

The simulation results in Fig.5-16 ~Fig.5-18 agree with Fig.2-5. The relaxation oscillation frequency increases with the increase of the laser output power which is almost the power of main mode. The performance of RIN also increases with the increase of the power of ASE since mode partition noise and mode hopping noise get even more suppressed.

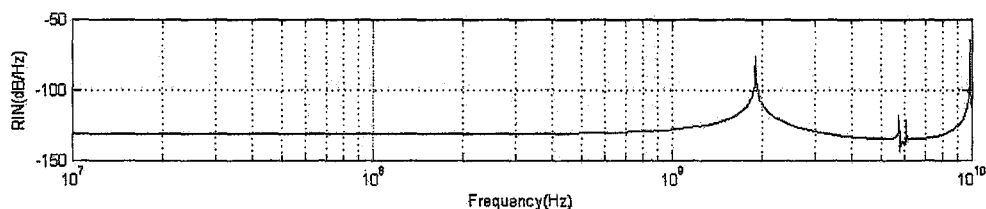


(Fig. 5-16 RIN in the injection locked F-P LD with -18.5dBm ASE injection)

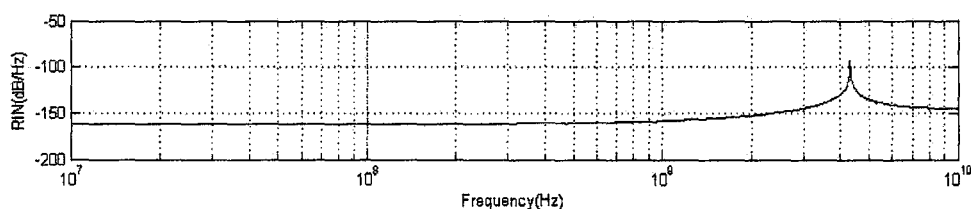


(Fig.5-17 RIN in the injection locked F-P LD with -10dBm ASE injection)

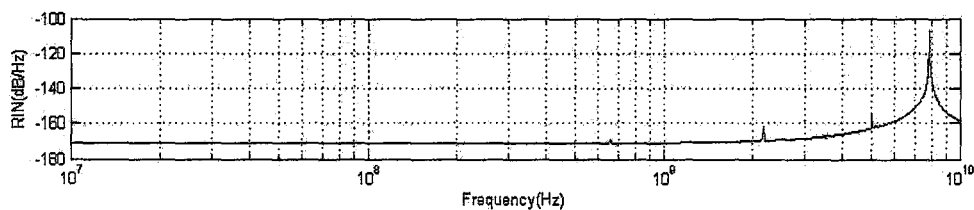


(Fig. 5-18 RIN in the injection locked F-P LD with -3dBm ASE injection)

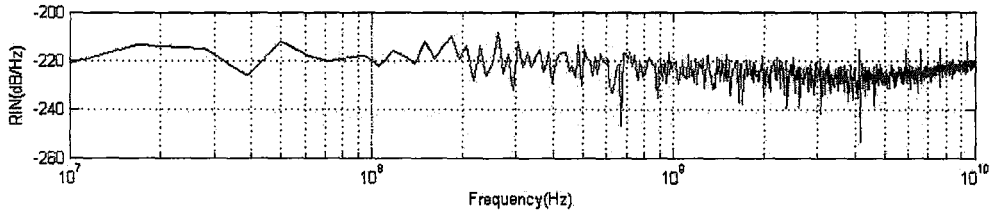


(Fig.5-19 RIN in the injection locked F-P LD with 10dBm ASE injection)

After injected by a high power ASE signal, F-P LD cannot be described precisely by RE model.

The simulation results about RIN agree with Fig.2-9.

(3) Gain

Since nonlinear effect is considered in the simulation, gain decreases with the increase of electrical field, in other words, with the increase of photon density. Photon population in all modes remains zero for a time period known as the turn-on delay time after which it increases rapidly. Relaxation oscillation takes several nanoseconds to become sufficiently damped for mode intensities to reach their steady-state values. With the small signal injected, photon density doesn't change a lot then neither does gain (see Fig.5-20~Fig.5-22). Gain decreases obviously after a rather big signal injected which is much close to the injection locked area (See Fig.5-23).

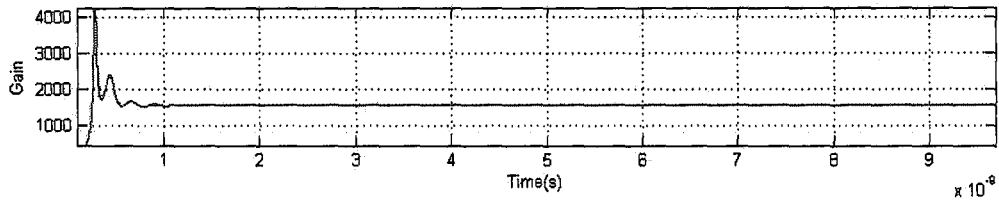


(Fig.5-20 Gain in the free running F-P LD)

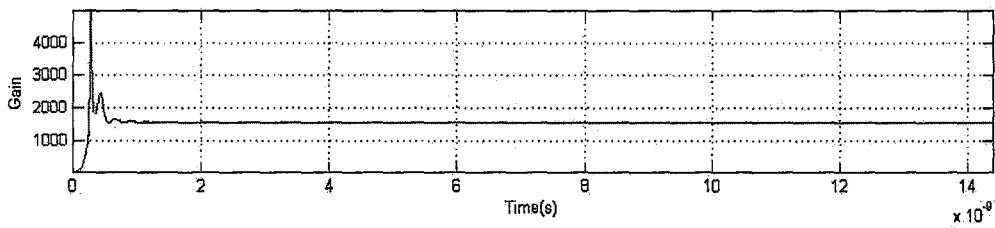


(Fig.5-21 Gain in the injection locked F-P LD with -50dBm ASE injection)

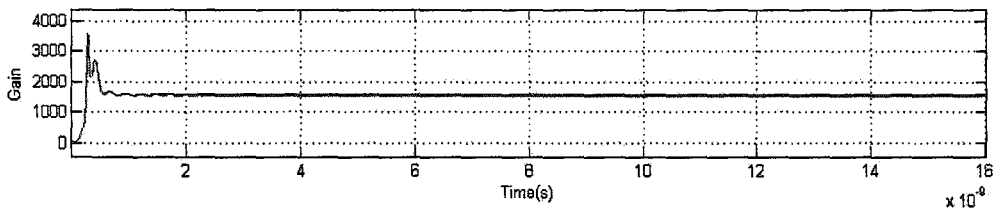


(Fig.5-22 Gain in the injection locked F-P LD with -35dBm ASE injection)

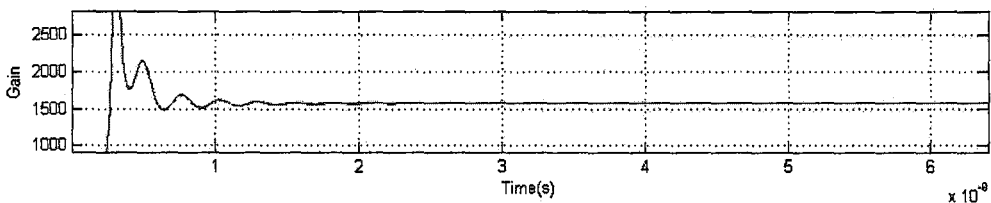


(Fig.5-23 Gain in the injection locked F-P LD with -18.8dBm ASE injection)

When F-P LD works in the injection locked area, master laser quenches all the side mode and forces slave laser oscillates in the single mode status. And the linearized gain (see equation (59)) explains dynamic characteristics about gain well when we assume that the laser operation is not so far from the laser threshold (see Fig. 5-23~Fig.5-25).

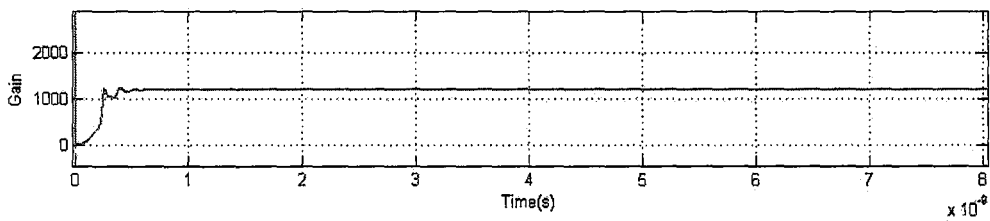


(Fig.5-24 Gain in the injection locked F-P LD with -18.5dBm ASE injection)

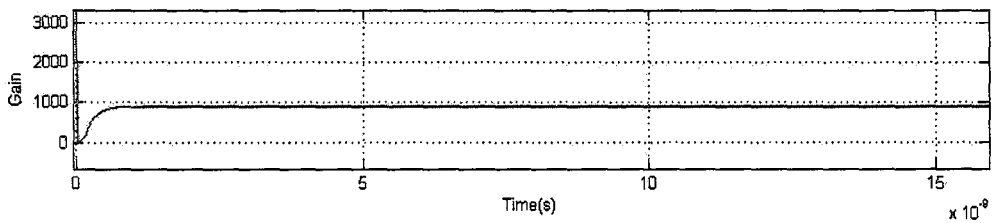


(Fig.5-25 Gain in the injection locked F-P LD with -10dBm ASE injection)

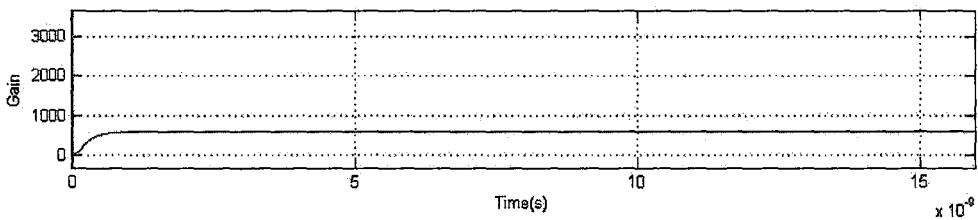


(Fig.5-26 Gain in the injection locked F-P LD with -3dBm ASE injection)

However, by injected a big ASE light signal, equation (59) cannot explain well. In this case, F-P model predicts a wider locking bandwidth so is more useful for large signal. (see Fig.5-27).

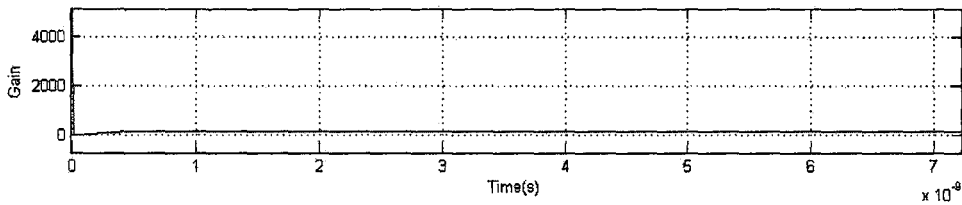


(Fig.5-27 Gain in the injection locked F-P LD with 10dBm ASE injection)

5.3 Summary

Our goal is to find out a cost efficient way to realize wavelength independent transceiver in ONU. We theoretically analyzed the F-P LD injected locked by sliced broadband light source based on RE model. The simulation results show that the injection locked F-P LD with NASE emits a very good longitudinal single mode characteristic so could be used in the reflective architecture of WDM-PON as a good solution of wavelength independent transmitter in ONU.

Chapter6. Summary and Future Work

The overall objective of this study is to find out a cost effective way to establish WDM-PON broadband access network.

In this thesis, we are actually dealing with a kind of reflective architecture in which all of the individual wavelengths of ONU are provided by a shared network resource (see Fig.3-1).A shared network source is used to seed the return path modulators with the end user's ONU. The upstream transmitter within the ONU only requires an identical reflective optical modulator.

We study the ASE of an EDFA as the broadband seed light source and F-P LD as the reflective optical modulator. The sliced continuous wave ASE (cw) seed light is used to injection lock an F-P LD transmitter in ONU. From the injection locked point of view, the ASE light is the master laser and F-P LD is the slave laser. So this is not the same as coherent injection locked of two lasers anymore. Our work is to explain this phenomenon theoretically by solving the rate equation.

In this scheme one F-P cavity mode which falls within the spectral pass band of the filter will be amplified and modulated by the ONU laser and returned back through the filter. Resonant operation of the reflective transmitter reduces the required drive current and can reduce the slicing noise through gain saturation.

The laser is different from normal F-P transmission lasers because the laser chip should have lower than normal reflectivity on the front facet and enhanced reflectivity on the back facet. The chip should also be longer than a conventional F-P LD to reduce the cavity mode spacing to enable more laser longitudinal modes to fall within the spectral pass band of the filter such as an AWD. This effect can reduce the impact of mode competition noise. In the simulation we ignore the mode partition noise. To optimize the performance of the injection locked scheme required control of both the laser parameters and the injected optical power. The optimization of the operation point will also be dependent on the position of the natural gain peak of the laser compared to the injected spectral slice so is likely to vary between ONU's.

So in the first chapter we study some fundamentals about WDM-PON in order to find a cost effective way to implement it. In the second chapter we study the characteristics of F-P LD and injection locked F-P LD in order to theoretically analyze how to choose the parameters of an F-P LD. In the third chapter we study one effective seed light source. In the fourth chapter we study some good experiments about injection locked F-P LD with NASE in WDM-PON reflective architecture. In the fifth chapter we setup one F-P LD model based on experiments from chapter three and theoretical analysis from chapter two and simulate the dynamic characteristics of injection locked F-P LD by numerically solving the rate equation. The simulation results agree with experimental results.

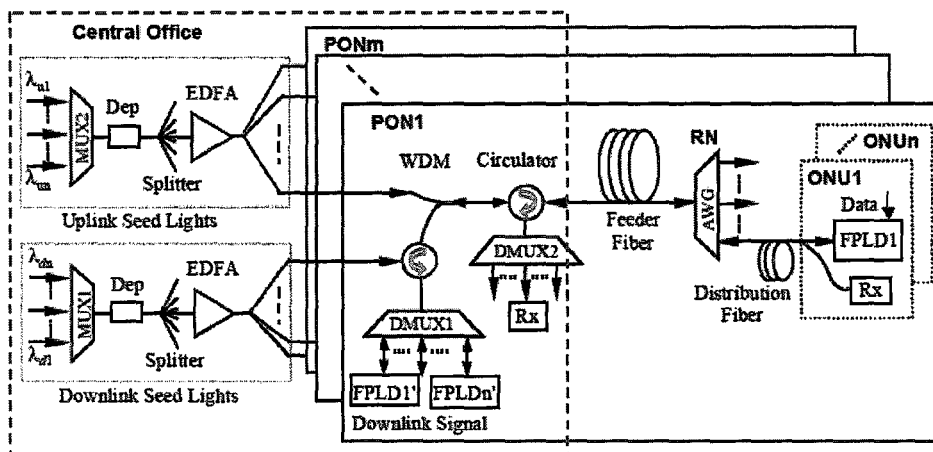


(Fig.6-1 Proposed WDM-PON architecture using CW-injection-locked F-P LD)

However, there is still a lot of work to do. Using F-P LD injection-locked by spectrum-sliced broad-band incoherent light source, the user bandwidth is limited because of the conversion of excess intensity noise (IN) from the seed light to the FP-LDs. In order to further increase the data rate, the use of high-quality seed light sources with low IN is essential. The experiment [24] shows that by using F-P LD injected locked by continuous wave coherent seed light the IN can be largely eliminated and user bandwidth can be improved to 10GHz with the transmission error free.

The later work should be to construct more precise theoretical model based on those more complex experiments.

References

1. ITU-T Recommendation G.984.1: General characteristics for Gigabit-capable Passive Optical Networks
2. Alex Vukovic, Khaled Maamoun, Heng Hua, Michel Savoie, Performance Characterization of PON Technologies: Broadband Applications and Optical Networks, Communications Research Centre (CRC) ;Ottawa ;ON,Canada,K2H8S2
3. www.ciphotonics.com : WDM-PON technologies
4. www.corning.com
5. C.H.Henry, Theory of the line width of semiconductor lasers, IEEE Journal of Quantum Electronics
6. <http://cp.literature.agilent.com/litweb/pdf/5091-2196E.pdf>
7. Ohtsubo, Junji: Semiconductor Lasers [electronic resource]: Stability, Instability and Chaos, 2008. Published by Berlin, Heidelberg: Springer-Verlag
8. G.P.Agrawal and N.K.Dutta: Semiconductor Lasers, 2nd ed. New York: Van Nostrand, 1993.
9. Reuven Gordon, Fabry–Perot Semiconductor Laser Injection Locking, IEEE Journal of Quantum Electronics, VOL. 42, NO. 4, April 2006
10. M. M. Ibrahim and M. S. Ibrahim, A comparison between rate-equation

- and fabry-perot amplifier models of injection locked laser diodes,
Opt.Laser Technol., VOL. 28, and NO. 1, pp. 39–42, 1996.
11. Marcuse D., Lee TP, On approximate analytical solutions of rate equations for studying transient spectra of injection lasers, IEEE Journal of Quantum Electronics, Sep 1983, VOL: 19, pp: 1397- 1406
 12. Otsuka K. and Tarucha S., Theoretical Studies on Injection Locking and Injection-Induced Modulation of Laser Diodes, IEEE Journal of Quantum Electronics, VOL. QE-17, NO. 8, AUGUST 1981
 13. Iwashita K. and Nakagawa K., Suppression of mode partition noise by laser diode light injection, IEEE Journal of Quantum Electronics 1982, QE18, pp. 1662-1674
 14. Lidoyne P., Gallion C., Chabran G. and Debarge, Locking range, phase noise and power spectrum of an injection-locked semiconductor laser, IEEE Proceedings, VOL. 137, Pt. J, NO. 3, June 1990
 15. L. Li, Static and dynamic properties of injection-locked semiconductor lasers, IEEE Journal of Quantum Electronics, VOL. 30, NO. 8, pp. 1701–1708, Aug. 1994.
 16. Dag Roar Hjelme and Alan Rolf Mickelson, Gain nonlinearities due to carrier density dependent dispersion in semiconductor lasers, IEEE Journal of Quantum Electronics, VOL.25.NO.7,JULY 1989
 17. K Petermann, Laser Diode Modulation and Noise, 1988
 18. Roy Lang, Injection Locking Properties of a Semiconductor Laser, 1982

IEEE

19. Nikolaus Schunk and Klaus Petermann, Noise Analysis of Injection-Locked Semiconductor Injection Lasers, IEEE Journal of Quantum Electronics, VOL. QE-22, NO. 5, MAY 1986
20. Xiaofei Cheng, Yang Jing Wen, Zhaowen Xu, Yixin Wang, Junhong Ng, Jaya Shankar, Network Technology Department, Institute for Infocomm Research (I2R), A-STAR, Singapore and Wanyi Gu, Jie Zhang, Optical Communication Centre, Beijing, Study on Spectrum Sliced ASE Source for Injection-locking of Fabry-Perot Laser Diodes
21. H.D.Kim, S.-G.Kang, and Chang-Hee Lee, A Low-Cost WDM Source with an ASE Injected Fabry-Perot Semiconductor Laser, IEEE Photon. Technol. Lett., VOL. 12, NO.8, pp. 1067-1069, Aug. 2000
22. Tae-Won Oh, Jin-Serk Baik, Jae-Ho Song and Chang-Hee Lee, Broadband Light Source for Wavelength-Division Multiple Access Passive Optical Network
23. K.Park, S.Mun, K.Choi and C. Lee, A theoretical model of a wavelength-locked Fabry-Perot Laser Diode to the externally injected narrow-band ASE, IEEE, Photon. Technol. Lett., VOL 17, NO.9, pp. 1797-1799, September, 2005
24. Kun-Youl Park, Chang-Hee Lee, Intensity Noise in a Wavelength-Locked Fabry-Perot Laser Diode to a Spectrum Sliced ASE, IEEE Journal of Quantum Electronics, VOL., 44, NO.3, MARCH 2008

25. S.C. Woodworth, D. T. Cassidy, and M. J. Hamp, Experimental analysis of a broadly tunable InGaAsP laser with compositionally varied quantum wells, *IEEE Journal of Quantum Electronics*, VOL. 39, NO. 3, pp. 426–430, Mar. 2003.
26. M. J. Hamp and D. T. Cassidy, Critical design parameters for engineering broadly tunable asymmetric multiple quantum well lasers, *IEEE Journal of Quantum Electronics*, VOL. 36, NO. 8, pp. 978–983, Aug. 2000.
27. E. H. Lee, Y. C. Bang, J. K. Kang, Y. C. Keh, D. J. Shin, Member, IEEE, J. S. Lee, S. S. Park, I. Kim, Member, IEEE, J. K. Lee, Y. K. Oh, and D. H. Jang, Uncooled C-Band Wide-Band Gain Lasers With 32-Channel Coverage and 20-dBm ASE Injection for WDM-PON, *IEEE Journal of Quantum Electronics*, VOL. 18, NO. 5, MARCH 1, 2006 667
28. G.H.B. Thompson, A theory of filamentation in semiconductor lasers including the dependence of dielectric constant on injected carrier density, *Opto-Electron.*, vol. 4, pp. 257-310, 1972